CHAPTER -III

RESULTS AND DISCUSSION

In this chapter, the results of characterization and catalytic activity of metal complexes supported on functionalized poly(styrene-divinylbenzene) is described. These polymer supported metal complexes have been examined as possible catalysts in the oxidation and hydrogenation of olefins. The chapter includes the results and discussion of :-

1. Polymer supported **Ru - Schiff base complexes**
2. Polymer supported **Fe - Schiff base complexes**
3. Polymer supported **2-aminopyridyl Ru- complexes**
4. Polymer supported **Pd - Schiff base complexes**

I. POLY(STYRENE-DIVINYLBENZENE) SUPPORTED RUTHENIUM(III) COMPLEXES

The chemical modification of crosslinked chloromethylated poly(styrene-divinylbenzene) and the loading of ruthenium onto this support was carried out as per the sequence shown in **Scheme 3.1**. The four catalysts studied are designated as under:

Ru - A : **8% Poly(S-DVB) Ru(III) (en-SB)**

Ru - B : **14% Poly(S-DVB) Ru(III) (en-SB)**

Ru - C : **8% Poly(S-DVB) Ru(III) (2ap-SB)**

Ru - D : **14% Poly(S-DVB) Ru(III) (2ap-SB)**

Catalyst Characterization

Physical properties of the newly synthesized catalysts **Ru-A - Ru-D** and the microanalysis at different stages of preparation are presented in **Tables 3.1** and **3.2**. The surface area of catalysts **Ru-C** and **Ru-D** bearing 2-amino pyridine Schiff bases (46.17 and 48.31 m^2g^{-1}) are found to be lower than those derived from ethylene diamine[**Ru-A** (62.69 m^2g^{-1}) and **Ru-B** (61.29 m^2g^{-1})]. This difference of 13-16 m^2g^{-1} is probably due to the relative size difference in the two types of Schiff bases formed on the polymer matrix.

The attachment of Schiff base derived from ethylenediamine and 2-aminopyridine on the functionalized polymer was confirmed by their elemental analysis. The higher percentage of nitrogen found in **Ru-A** and **Ru-C** compared to that in **Ru-B** and **Ru-D** is attributed to the lower degree of cross linking in the former (8% in **Ru-A** and **Ru-C** as against 14% in **Ru-B** and **Ru-D**). This can be explained as follows. In the case of polymer supports with a higher degree of cross linking, the network has a dense and relatively larger number of inaccessible domains resulting in less functionalization [1].

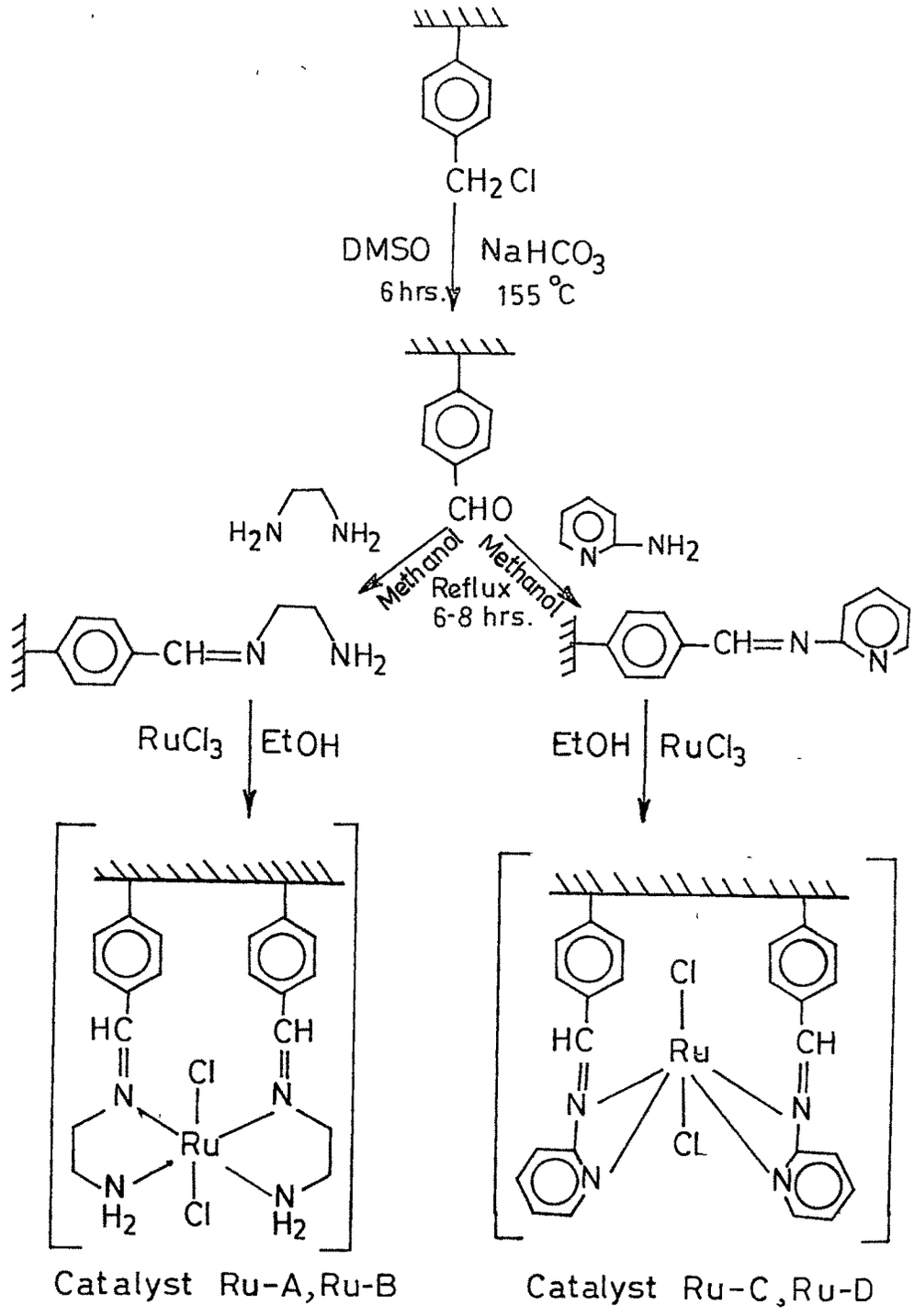

Scheme 3.1 : Synthesis of polymer supported Ru(III)-Schiff base complexes

Table 3.1
Elemental analysis of chloromethylated polymers, their Schiff bases and supported Ru(III) catalysts

Compound	C%	H%	Cl%	N%	Ru (mmol /g resin)
8% P(S-DVB)CH_2Cl	67.62	5.67	22.32	---	---
14% P(S-DVB)CH_2Cl	81.79	7.03	14.21	---	---
8% P(S-DVB)(en-SB)	76.55	7.08	---	3.03	---
14% P(S-DVB)(en-SB)	84.72	7.46	---	1.84	---
8% P(S-DVB)(2ap-SB)	72.41	6.29	---	1.12	---
14% P(S-DVB)(2ap-SB)	82.84	7.13	---	1.05	---
Ru-A	73.79	6.65	---	2.61	$8.1x10^{-3}$
Ru- B	84.28	7.48	---	1.58	$9.2x10^{-3}$
Ru- C	74.66	6.32	---	0.71	$3.6x10^{-3}$
Ru- D	81.26	7.48	---	0.44	$7.8x10^{-3}$

Table 3.2
Physical properties of polymer-supported Ru(III) catalysts

Property	Catalyst			
	Ru-A	Ru-B	Ru-C	Ru-D
Surface area($m^2 g^{-1}$)	62.69	61 29	46.17	48.31
Moisture content (wt%)	2.79	1.04	2.86	0.72
Bulk density ($g\ cm^{-3}$)	0.44	0.43	0 45	0.43
Pore volume ($cm^3 g^{-1}$)	0.33	0 33	0.21	0.32

Table 3.3
Swelling data of supported catalysts (mol%)

	Catalyst			
Solvent	Ru-A	Ru-B	Ru-C	Ru-D
water	5.27	5.50	5.36	5.82
ethanol	2.05	2.12	2.30	2.21
methanol	2.92	3.05	3.20	3.62
acetonitrile	2.30	2.40	3.06	2.43
benzene	1.19	1.25	1.06	1.07
THF	1.38	1.40	1 03	1.22
heptane	0.95	0.99	0.92	1.00

Polar solvents were generally found to be good swelling agents for all the catalysts than non-polar solvents like heptane, benzene etc. (**Table 3.3**). This is expected because with increase in the degree of cross-linking of the polymer support, the percent swelling decreases indicating the rigid nature of the support. Thus, the solvent of choice should combine good swelling ability and high polarity for catalytic use. Methanol was found to be a good solvent among those studied and exhibited better property for dissolution of the substrate.

The mid i.r. (4000-400 cm^{-1}) and far i.r. spectra (500-50 cm^{-1}) of polymer supported ruthenium complexes at different stages of synthesis (**Scheme3.1**) were recorded to know the nature of coordination of the metal to the polymer **Figs. 3.1a - 3.1e**. A strong band in the range of 1690 -1640 cm^{-1} ascribed to the C=N stretching (azomethine) in case of the Schiff base bearing polymer undergoes a downward shift with slight reduction in intensity in the supported metal catalysts. This indicates coordination of the ligand nitrogen (through the azomethine 'N') to the Ru(III) metal ion which is further supported by the Ru-N and Ru-Cl stretching vibrations which appear in the region 280-380 cm^{-1} in all catalysts[2-3]. These new bands in the far i.r. spectrum of the Ru-complexes are not seen in the starting ligands. Some of the important i.r spectral bands are given in **Table 3.4.**

The uv-vis reflectance spectra of the newly synthesized catalysts in $BaSO_4$ matrix exhibit two weak intensity absorption bands in the region 350 nm and 420 nm respectively **(Fig. 3.2)**. The absence of characteristic strong ligand-metal charge transfer (LMCT) bands indicate that the latter absorption may be due to d-d transition of Ru^{+3} [4].

Scanning electron micrographs (SEM) of polymeric Schiff base ligands and their ruthenium complexes show that the unsupported catalysts have a smooth spherical structure. The loading of ruthenium metal onto the surface appears to be fine which could be observed at high resolutions. Energy dispersive x-ray studies (EDXA) also indicated changes in the

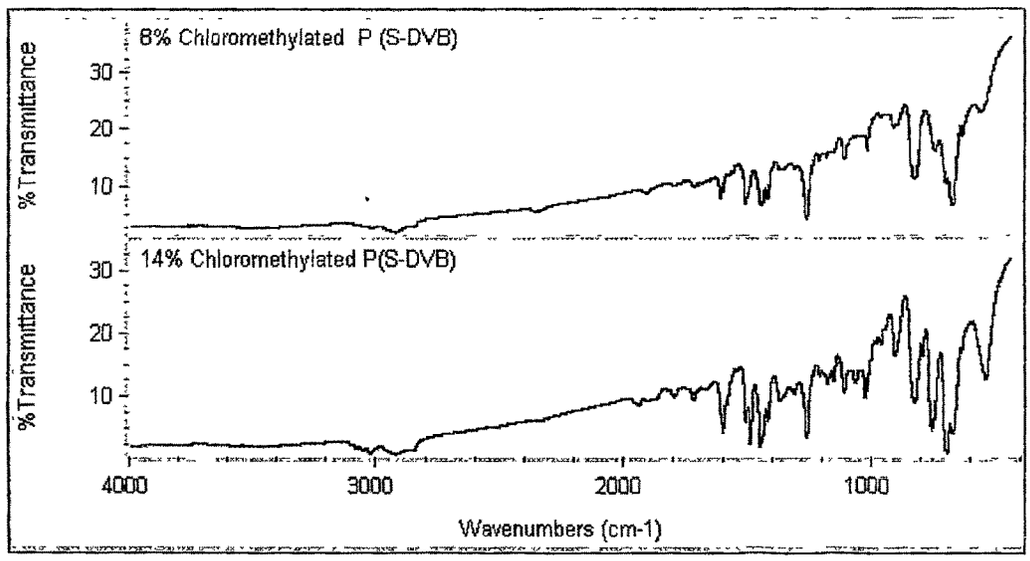

Fig. 3.1a : I.R. spectra of 8% and 14% chloromethylated P (S-DVB)

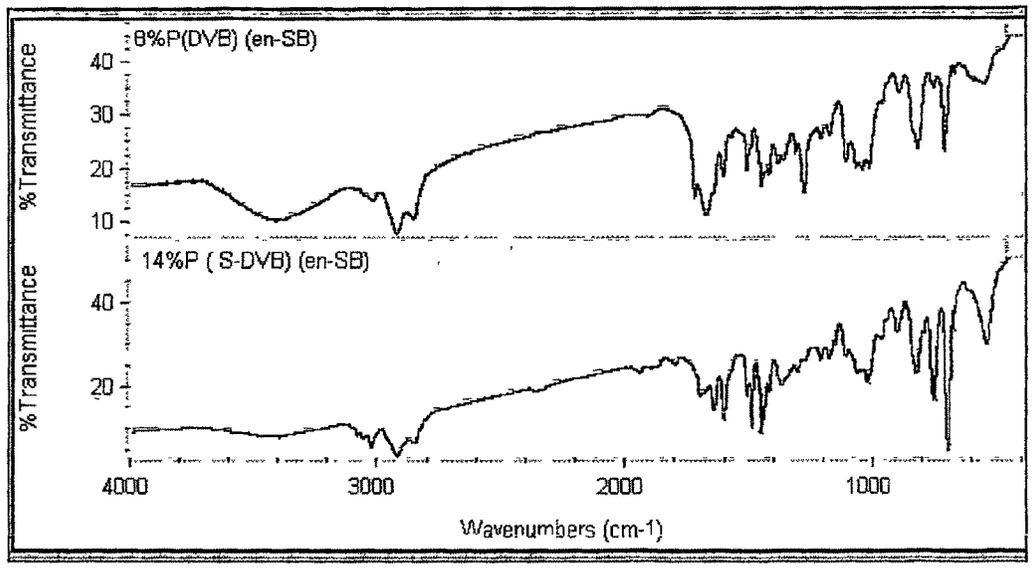

Fig. 3.1b : I.R. spectra of 8% and 14% P(S-DVB) (en-SB)

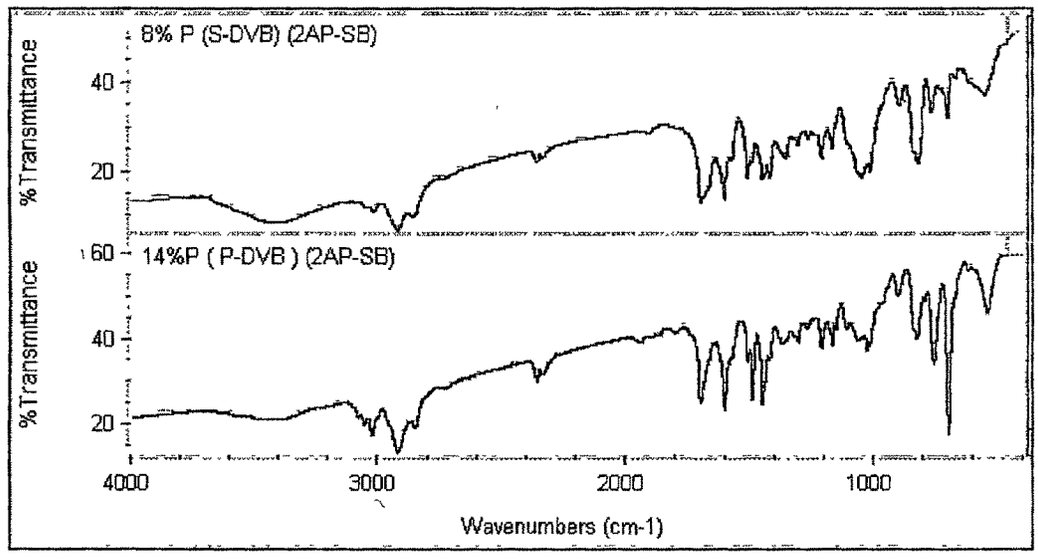

Fig. 3.1c : I.R. spectra of 8% and 14% P(S-DVB) (2ap-SB)

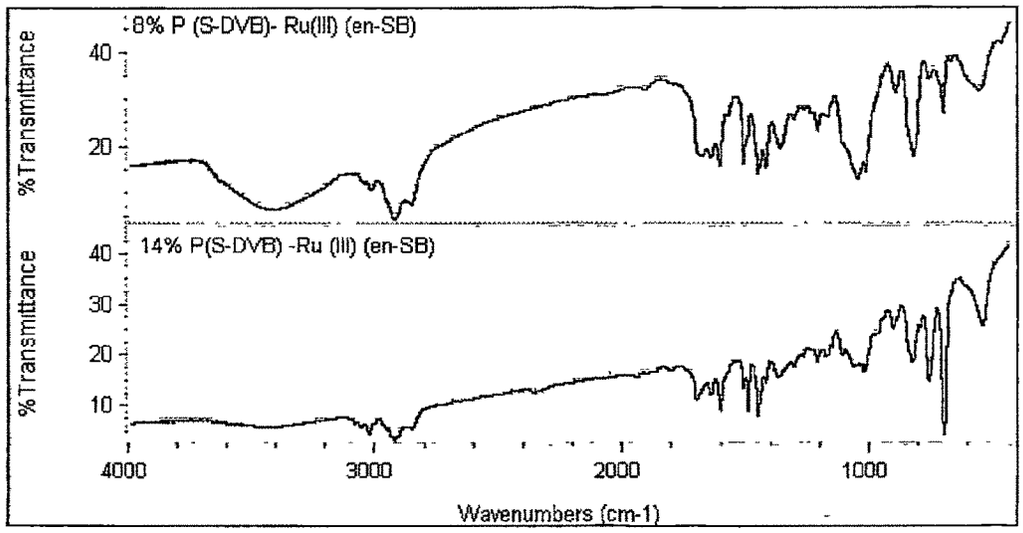

Fig. 3.1 d : I.R. spectra of 8% and 14% P(S-DVB) Ru (III) (en-SB) [Ru-A and Ru- B]

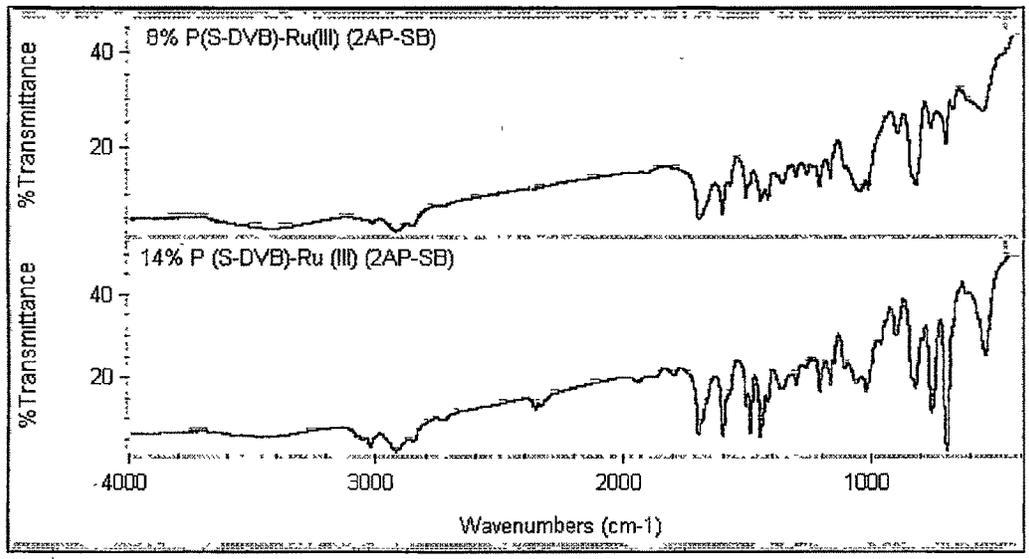

Fig. 3.1 e : I.R. spectra of 8% and 14% P(S-DVB) Ru (III) (2ap-SB) [Ru-C and Ru-D]

Table 3.4
I.r. spectral data of poly(styrene-divinylbenzene)-Schiff bases and their Ru(III) complexes

Compound	νNH cm^{-1}	νC=N cm^{-1}	νpyridyl ring cm^{-1}	νM-N cm^{-1}	νM-Cl cm^{-1}
8%P(S-DVB(en-SB)	3419br	1672s			
14%P(S-DVB)(en-SB)	3430br	1676s			
8%P(S-DVB)(2ap-SB)	3429br	1699s	1215ms 1169ms		
14%P(S-DVB)(2ap-SB)	3436br	1699s	1165ms 1215ms		
Ru-A	3409br	1648ms		383w	278w
Ru-B	3430br	1646ms		377w	282w
Ru-C	3423br	1686ms	1170ms 1216ms	375w	280w
Ru- D	3432br	1690ms	1175ms 1222ms	374w	281w

s = strong ; m = medium; br = broad; w = weak

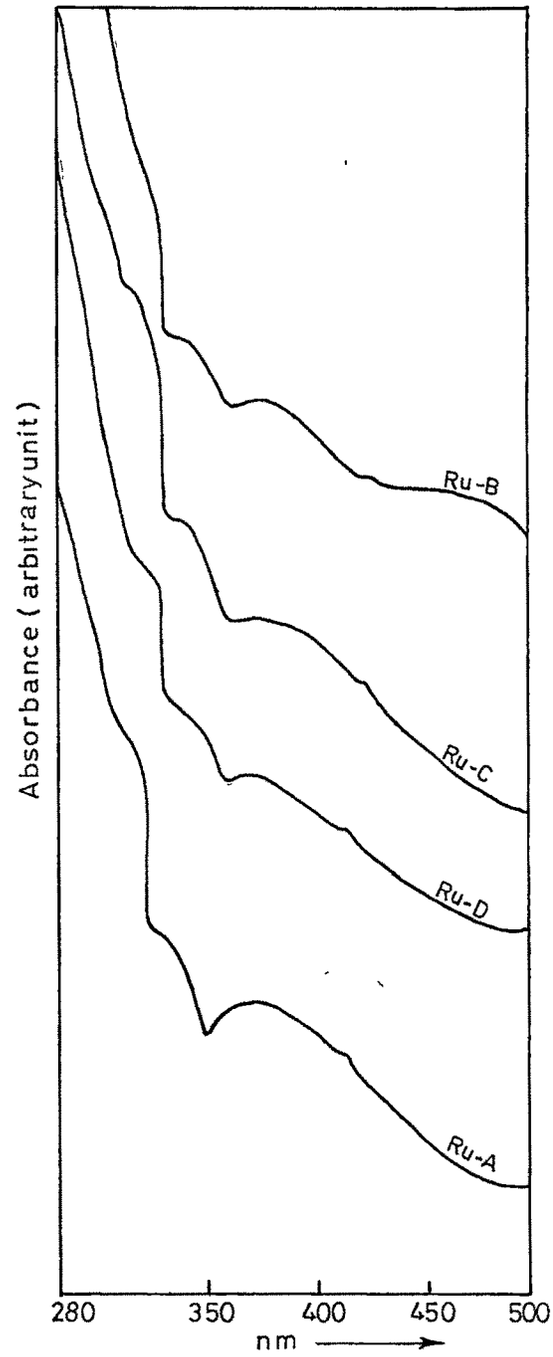

Fig 3 .2 : UV-VIS spectra of Ru(III)-Schiff base complexes

morphology of the supported catalysts. Representative SEM micrographs are shown in **Plate3.1a - b**. However, it is difficult to draw definite conclusion regarding the concentration changes of the metal across the surface of the fresh catalyst and the spent catalyst, probably due to very low concentration of metal which was generally in the range of 0.5 x 10^{-4} mmol Ru g^{-1} resin for our system.

Thermogravimetric analysis (TGA) of the unsupported polymers indicate degradation at lower temperatures compared to the ruthenium anchored polymer (**Table 3.5**). The lower stability of the metal supported polymers is also revealed by higher weight loss which may be due to dissociation of the Schiff base ligand moieties from the catalyst. Typical thermograms are shown in **Figs.3.3 –3.5.**

Catalytic Activity

Tertiary butyl hydroperoxide (TBHP, t-BuOOH) was used as the terminal oxidant in the epoxidation of *cis*-cyclooctene and styrene in presence of catalyst **Ru-A - Ru-D** at room temperature and at 50°C. Control experiments showed that the alkenes did not undergo epoxidation in the absence of either the catalyst or oxidant. When molecular oxygen was used as the source of oxidant in place of TBHP practically no reaction occurred. The results of epoxidation of cyclooctene and styrene in acetonitrile and methanol using supported Ru catalysts are compiled in **Tables 3.6** and **3.7**.

Analysis of oxidation products showed that in case of *cis*-cyclooctene, the corresponding epoxide was selectively formed. Epoxide yields increased substantially at 50°C than at 26°C (**Table 3.6**). From the data obtained it appears that the observed selectivities and yields are comparable to other mononuclear and binuclear Ru(III)-Schiff base complexes[5-9]. Direct comparison of activity of homogeneous Ru(III) complexes with Schiff base ligands used in the present study would reflect the actual catalytic efficiency of

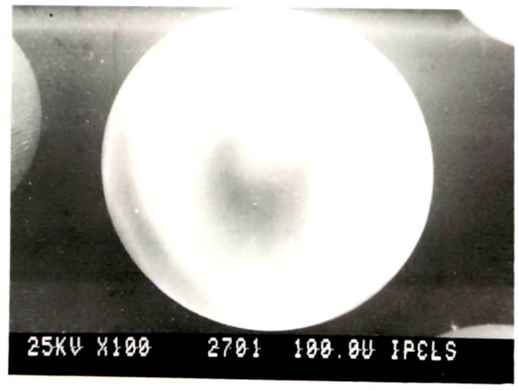

a

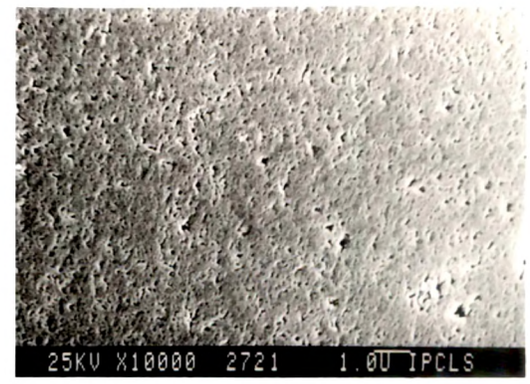

b

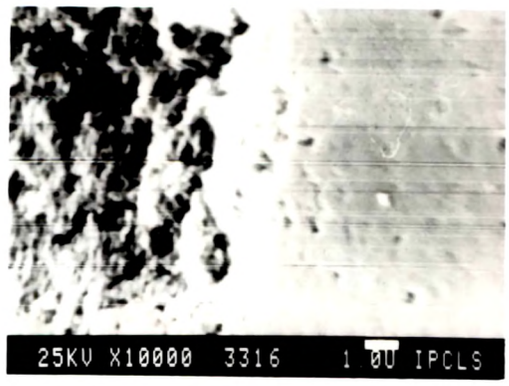

c

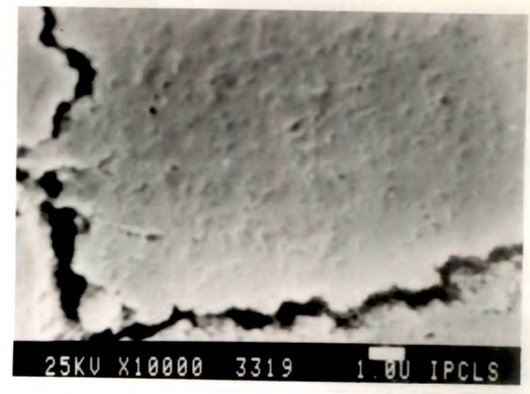

d

Plate 3.1 a : Scanning electron micrographs of (a,b) chloromethylated P (S-DVB) (c) P (S-DVB) (en-SB) (d) P (S-DVB) (2ap-SB)

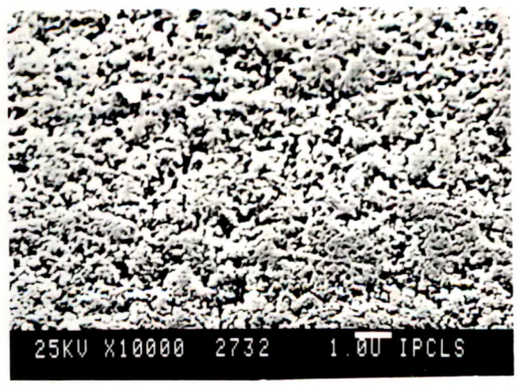

a

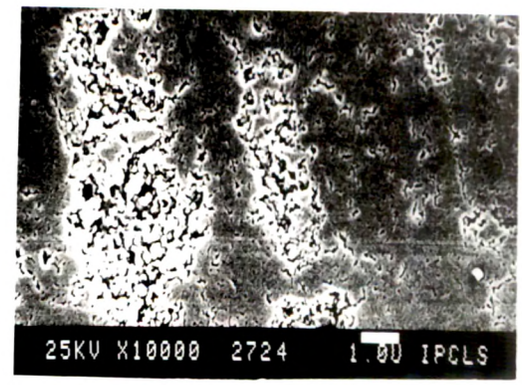

b

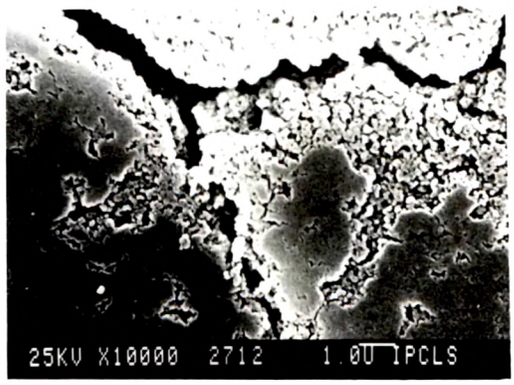

c

d

Plate 3.1 b : Scanning electron micrographs of (a) Ru-A (b) Ru-B (c) Ru-C (d) Ru-D

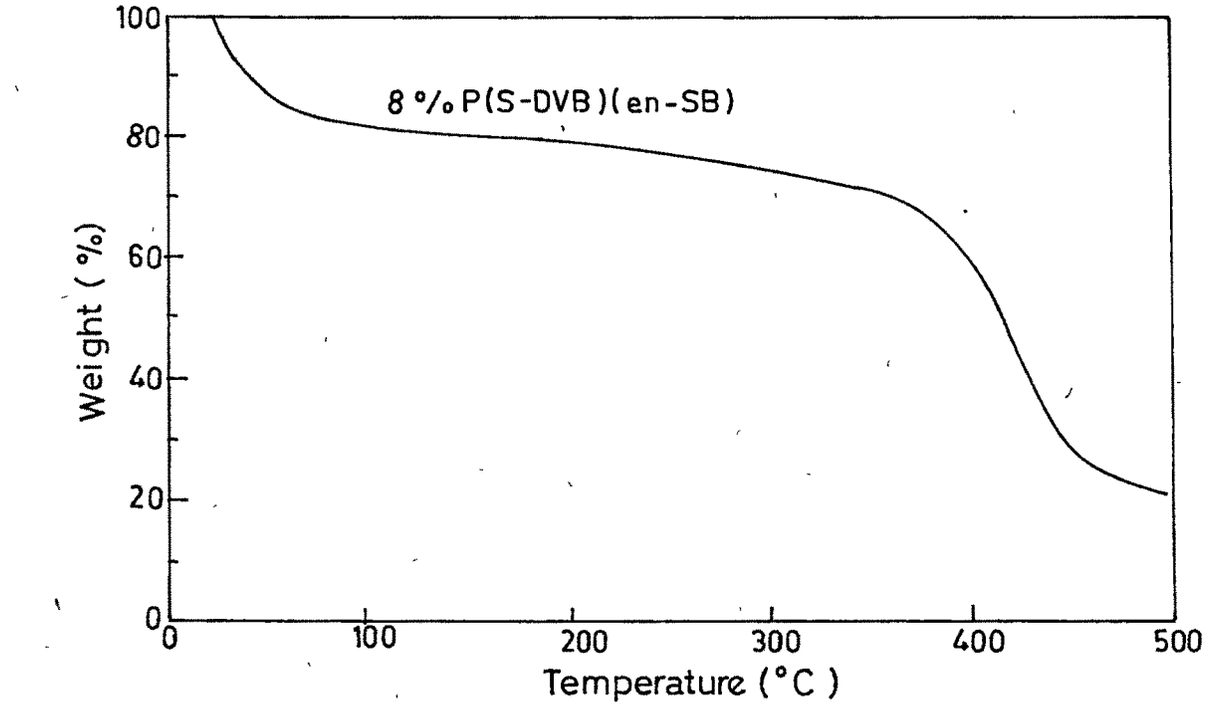

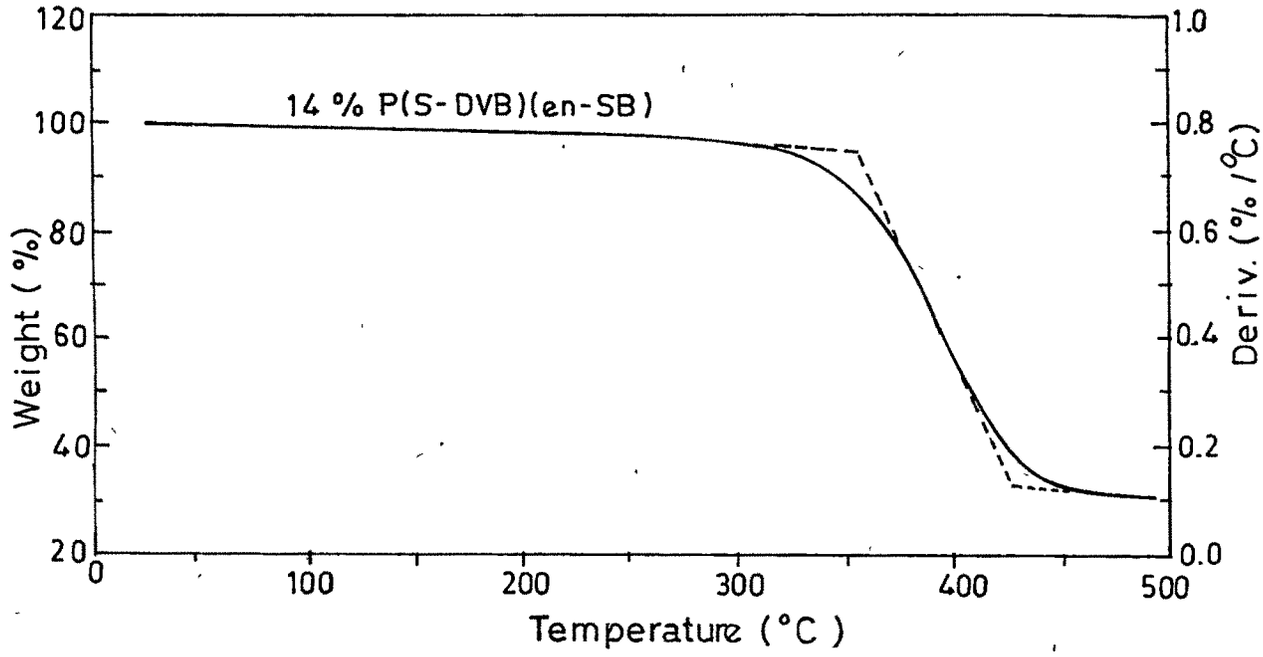

Fig. 3.3. Thermograms of polymer supported ethylenediamine- Schiff base

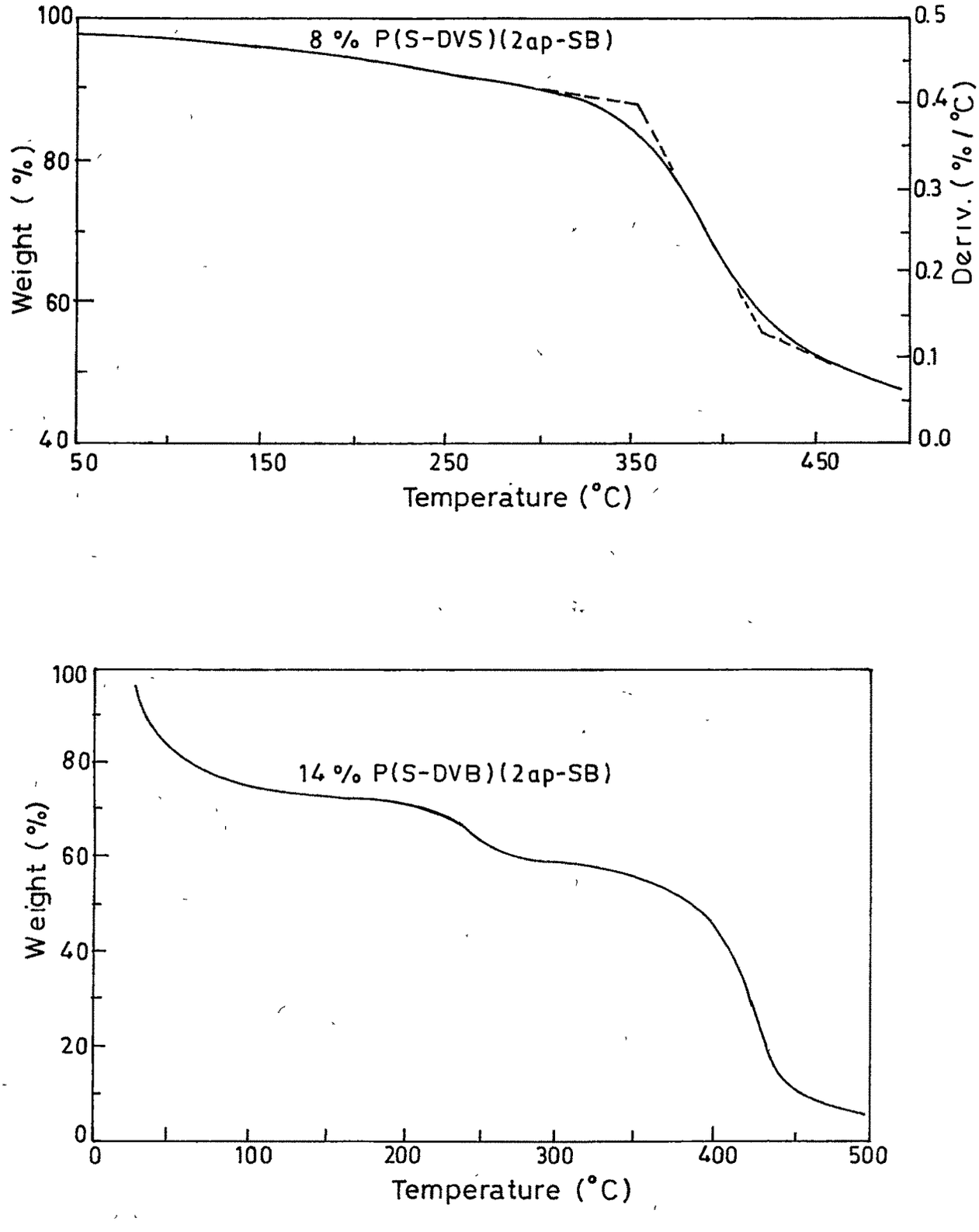

Fig. 3.4. Thermograms of polymer supported 2-aminopyridine - Schiff base

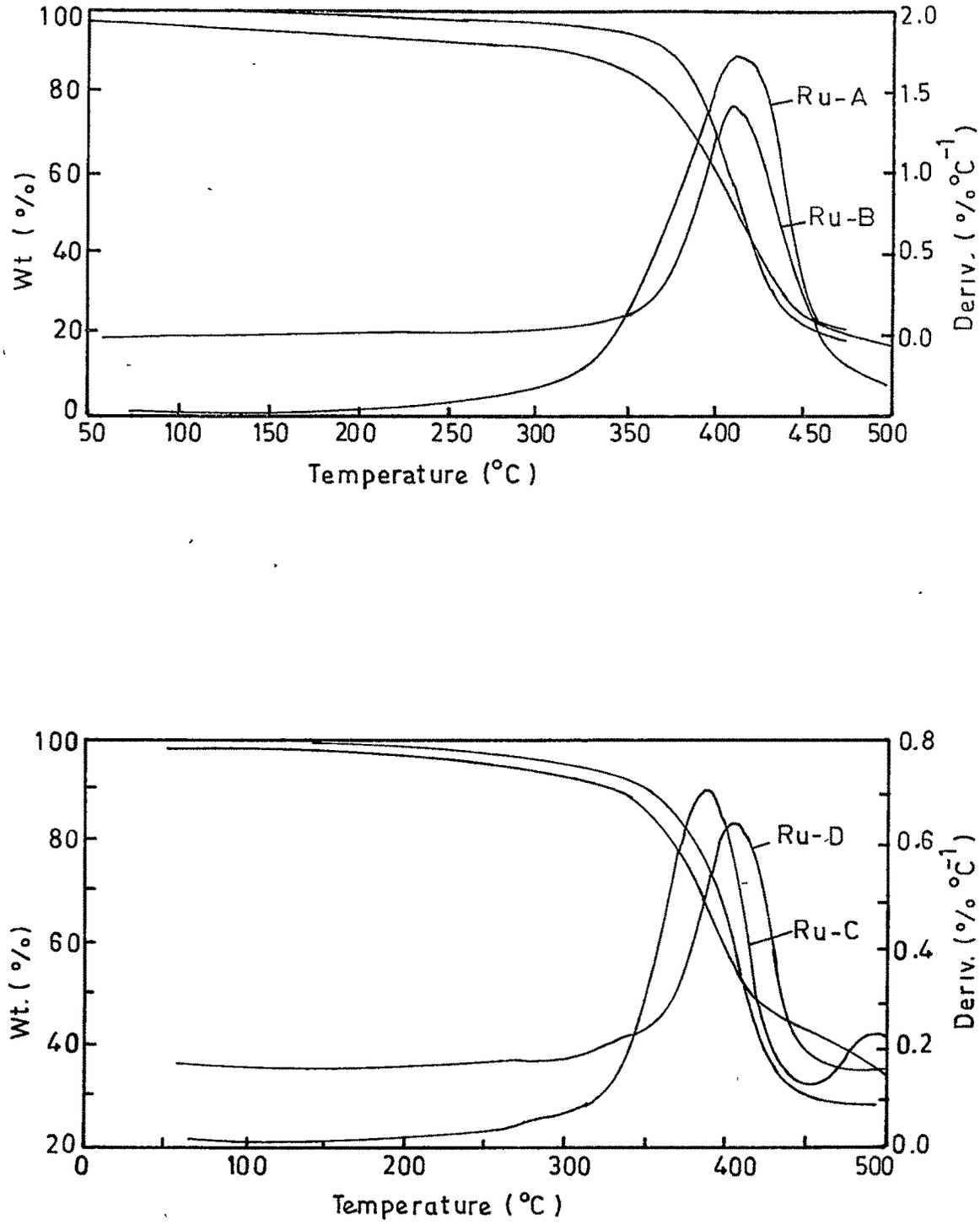

Fig 3.5 : Thermal analysis of polymer supported Ru(III)-Schiff base complexes

Table 3.5
T. g. data of polymer supported Schiff bases and their ruthenium complexes

Sample	Degradation temp(°C)	Wt.loss (%)
8% P(S-DVB)(en-SB)	412.9	47.2
14% P(S-DVB)(en-SB)	394.4	61.1
8% P(S-DVB)(2ap-SB)	378.9	32.7
14% P(S-DVB)(2ap-SB)	408.9	73.8
Ru-A	415.4	60.5
Ru-B	409.5	78.4
Ru-C	386.3	51.5
Ru-D	412.4	85.3

supported *vis-a-vis* unsupported catalysts under optimized reaction conditions However, data on the activity of the homogeneous ruthenium catalysts was presently, not available. Maximum activity was exhibited by **Ru-C** and **Ru-D** derived from 2-amino pyridine Schiff base (runs 7,8,15,16; **Table 3.6**). The degree of cross linking in the polymer support as well as the mode of binding of the Schiff bases (bidentate in case of 2-aminopyridine and monodentate or chelating in case of ethylenediamine) to the Ru(III) centre probably determines the relative activity of the catalysts during the epoxidation. Methanol was a better solvent compared to acetonitrile for oxidation under similar reaction conditions.

In case of styrene, interestingly, benzaldehyde as secondary oxidation product was formed in substantial quantities in addition to the expected styrene oxide (**Table 3.7**). This indicates that under the experimental conditions the reaction with TBHP proceeds beyond the epoxide stage resulting in oxidative cleavage of styrene. The other oxidation product phenyl acetaldehyde was not observed but small amount of acetophenone formation (< 0.3%) was detected. An increase in epoxide yield with temperature was noted for styrene also. From **Table 3.7** it can be inferred that the ability of the catalysts for oxidation of styrene is much higher than for cyclooctene.

A few experiments were carried out to determine the extent of epoxidation at different time intervals for oxidation of cyclooctene at 50°C (**Fig. 3.6**). In case of **Ru-B** and **Ru-C** the conversions reached a value of 23% and 26% in about 20hrs and reaches a plateau thereafter. With catalysts **Ru-A** and **Ru-D** the reaction proceeds slowly even after 24hrs, though there is no marked increase in yields (runs 13-16, **Table 3.6**). Though direct comparison of activity of present catalyst systems could not be made with analogous homogeneous Schiff base Ru(III) complexes, the trend in reactivity is comparable and in a few cases better performance was exhibited by supported catalysts (**Table 3.6**)[10]. A time *vs* % conversion is shown in **Fig. 3.6.**

Table 3.6
Epoxidation of *cis*-cyclooctene with polymer anchored Ru catalysts[a]

Run	Catalyst	Solvent	Temp. (°C)	Yield of epoxide (mmole)	Yield of epoxide[b] (%)
1	Ru-A	CH_3CN	26	0.43	4.3
2	Ru- B	CH_3CN	26	0.56	6.6
3	Ru-C	CH_3CN	26	0.62	7.4
4	Ru-D	CH_3CN	26	0.89	10.1
5	Ru-A	CH_3CN	50	1.03	12.1
6	Ru-B	CH_3CN	50	1.19	14.2
7	Ru-C	CH_3CN	50	2.52	29 5
8	Ru-D	CH_3CN	50	3.65	42.9
9	Ru-A	CH_3OH	26	0.20	4.9
10	Ru-B	CH_3OH	26	0.26	6.3
11	Ru-C	CH_3OH	26	0.52	12.6
12	Ru-D	CH_3OH	26	0.70	16.9
13	Ru-A	CH_3OH	50	0.98	20.9
14	Ru-B	CH_3OH	50	0.89	23.2
15	Ru-C	CH_3OH	50	1.15	27.6
16	Ru-D	CH_3OH	50	1.27	30.4

[a] *Conditions Weight of catalyst =0 25 g, cis-cyclooctene=10 mmol, TBHP= 4 mmol , time=24hrs*
[b] *yield based on oxidant taken*

Table 3.7
Epoxidation of styrene in presence of Ru-supported catalysts[a]

Run	Catalyst	Solvent	Temp. (^{0}C)	Styrene Oxide (mmole)	Styrene Oxide[b] (%)	Benzaldehyde (mmole)	Benzaldehyde[b] (%)
1	Ru-A	CH_3CN	26	0.20	4.8	0.21	4.9
2	Ru-B	CH_3CN	26	0.06	1.3	0.28	6.6
3	Ru-C	CH_3CN	26	0.08	1.7	0.32	7.5
4	Ru-D	CH_3CN	26	0.03	0.74	0.24	5.7
5	Ru-A	CH_3CN	50	0.73	17.2	3.46	81.6
6	Ru-B	CH_3CN	50	0.50	11.8	3.59	84.5
7	Ru-C	CH_3CN	50	1.10	26.0	3.12	73.5
8	Ru-D	CH_3CN	50	1.13	26.7	3.13	73.8
9	Ru-A	CH_3OH	26	0.07	1.8	0.95	22.4
10	Ru-B	CH_3OH	26	0.05	1.4	0.53	12.5
11	Ru-C	CH_3OH	26	0.27	6.4	0.86	20.4
12	Ru-D	CH_3OH	26	0.19	4.7	0.81	19.1
13	Ru-A	CH_3OH	50	0.33	7.8	1.19	28.1
14	Ru-B	CH_3OH	50	0.19	4.7	1.03	24.3
15	Ru-C	CH_3OH	50	0.20	28.4	1.55	36.5
16	Ru-D	CH_3OH	50	0.66	15.6	1.58	37.2

[a] *Conditions . Weight of catalyst= 0.25g; styrene=10 mmol; TBHP=4 mmol; time= 24hrs*
[b] *yield based on oxidant taken*

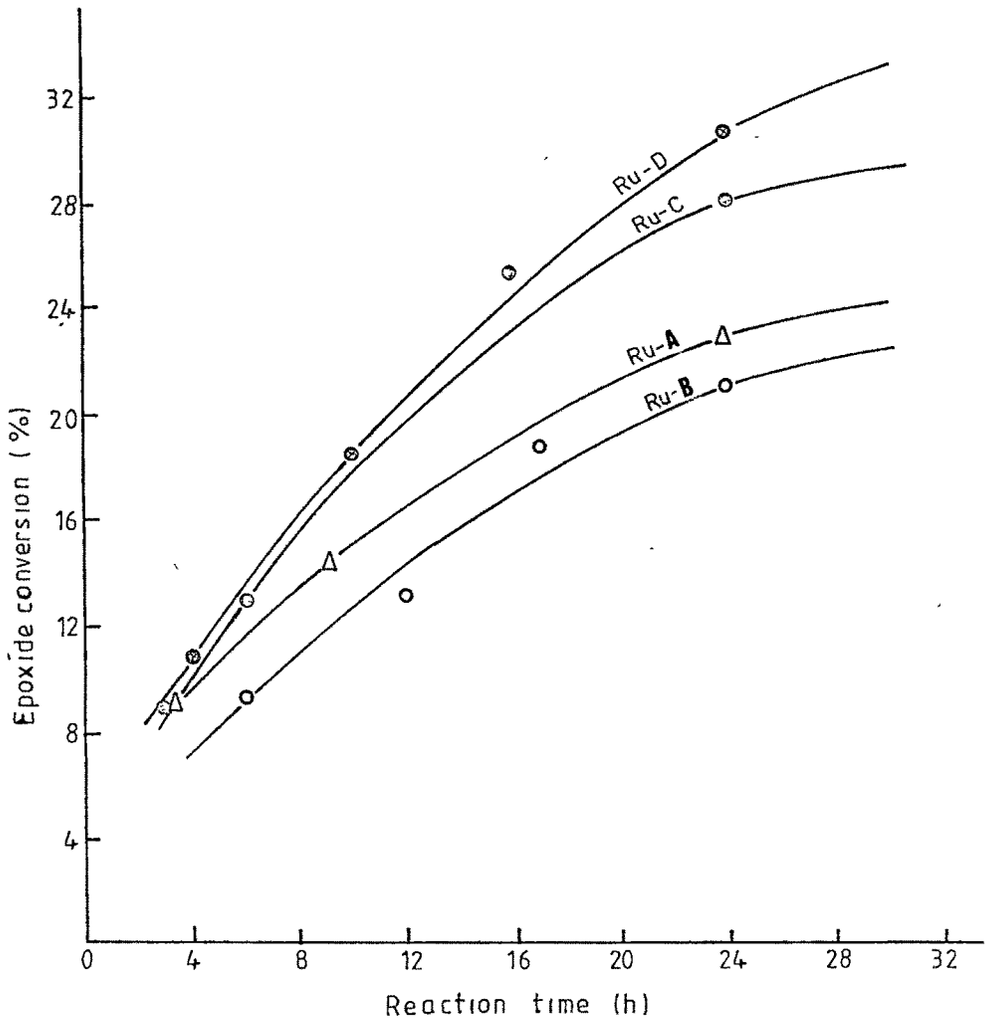

Fig 3.6 : Effect of reaction time on conversion of cyclooctene to epoxide in presence of t-BuOOH, , CH_3OH, 50°C , Ru(III) supported catalysts Ru-A (△) Ru-B(○) , Ru-C (●) , Ru-D (⊗).

II. POLY(STYRENE-DIVINYLBENZENE) SUPPORTED FE(III) SCHIFF BASE COMPLEXES

The Fe(III) complexes supported on modified polystyrene-Schiff bases (**Scheme 3.2**) were characterized by various physicochemical methods and evaluated for their activity in epoxidation of *cis*-cyclooctene and styrene. The different catalysts employed in this study are designated as under:

Fe-A : 8% Poly(S-DVB)Fe(III)(en-SB)

Fe-B : 14% Poly(S-DVB)Fe(III)(en-SB)

Fe-C : 8% Poly(S-DVB)Fe(III)(2ap-SB)

Fe-D : 14% Poly(S-DVB)Fe(III)(2ap-SB)

Catalyst Characterisation

The analytical data of the polymer bound complexes at different stages of preparation is presented in **Table 3.8**. The maximum Fe loading in the freshly prepared catalysts was found to be in the range of 5.3-8.0 mmol g^{-1} resin. Some of the important physical properties of the newly synthesized catalysts are provided in **Table 3.9**. The slightly higher surface area observed in both **Fe-C** and **Fe-D** than in **Fe-A** or **Fe-B** (difference of 2 - 3.8 m^2g^{-1}) may possibly be due to the relative differences in the size of Schiff base ligand of 2-aminopyridine and ethylenediamine[15]. The swelling behavior of the catalysts in polar and non-polar solvents are given in Table **3.10**. With an increase in crosslink density of the polymer the swellability decreases which is ascribed to the differences in the rigid network of the matrix Water exhibited higher percentage swelling however , for practical purposes, methanol and acetonitrile were used as the solvent of choice for carrying out catalytic reactions to overcome miscibility problem with the reactants.

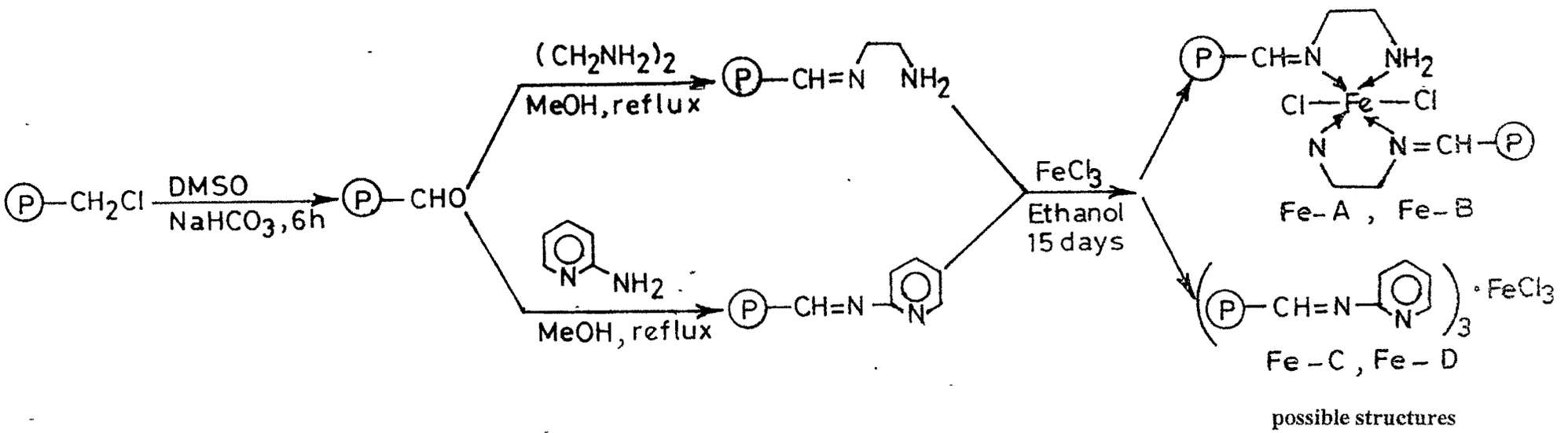

Scheme 3.2 : Synthesis of polymer supported Fe(III) -Schiff base complexes

Table 3.8
Elemental analysis at different stages of catalyst synthesis

Compound	C %	H %	N %	Fe (mmol /g resin)
8% P(S-DVB)-CHO	76.56	5.90	--	--
14% P(S-DVB)-CHO	86.20	7.29	--	--
8% P(S-DVB)-(en-SB)	72.35	7.07	6.20	--
14% P(S-DVB)-(en-SB)	84.64	7.56	1.86	--
8% P(S-DVB)- (2ap-SB)	75.80	6.74	2.58	--
14% P(S-DVB)-(2ap-SB)	83.88	7.31	2.07	--
Fe-A	69.70	6.86	5.86	7.68×10^{-5}
Fe-B	82.88	7.33	1.68	6.23×10^{-5}
Fe-C	75.86	6.81	1.22	5.34×10^{-5}
Fe-D	82.69	7.50	1.78	8.01×10^{-5}

Table 3.9
Physical properties of catalysts

Property	Fe-A	Fe-B	Fe-C	Fe-D
Surface area(m^2 g^{-1})	45.7	57.1	49.5	59.1
Moisture content(wt%)	2.2	1.9	1.9	1.7
Bulk density(g cm^{-3})	0.44	0.43	0.44	0.44
Pore volume(cm^{-3} g^{-1})	0.14	0.12	0.23	0.26

Table 3.10
Swelling studies of catalysts at 27°C(mol %)

Solvent	Fe-A	Fe-B	Fe-C	Fe-D
Water	5.4	5.3	5.4	5.3
Methanol	3.0	2.9	3.1	2.9
Ethanol	2.1	2.0	2.1	2.0
Acetonitrile	2.5	2.3	2.4	2.3
Benzene	1.3	1.2	1.2	1.2
Tetrahydrofuran	1.3	1.2	1.3	1.2
1,4-Dioxane	1.1	1.1	1.1	1.0
n-Heptane	0.9	1.0	1.0	0.9

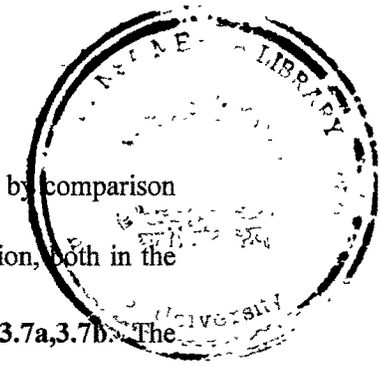

The mode of attachment of metal ion onto the support was confirmed by comparison of the i.r.spectral bands of the polymers before and after loading with Fe^{3+} ion, both in the mid ($4000cm^{-1}$- $400cm^{-1}$) and far ($600cm^{-1}$- $50cm^{-1}$) i.r. regions **Fig. 3.7a,3.7b**. The formation of Schiff base on the polymer support is indicated by a strong band appearing in the range of 1699-1646 cm^{-1} assigned to the C=N stretching frequency. This band shows a decrease in intensity and shift to lower wave numbers after complexation suggesting the co-ordination of the Schiff base to the central Fe(III) ion through the azomethine nitrogen. A medium intensity band at ~3400 cm^{-1} due to νNH of ethylenediamine containing ligand showed a marginal low frequency shift in the corresponding metal supported catalysts (**Fe-A** and **Fe-B**). In case of **Fe-C** and **Fe-D**, the pyridyl ring nitrogen stretching vibration of the Schiff base (780 cm^{-1}) shows a positive shift in the spectra of catalysts indicating co-ordination through the 'N' of pyridine. Low intensity bands were observed at 316 cm^{-1} and 385 cm^{-1} in the far i.r. spectra of all the catalysts. These bands which were not detected in the parent Schiff bases were assigned to νFe-N and νFe-Cl vibrations respectively (**Table 3.11**)[16,17]. However, due to the relatively low intensity bands in this region an unambiguous distinction between νFe-N(azomethine) and νFe-N(pyridyl) could not be made. Thus the structure of the complexes depicted in **Scheme 3.2** needs further confirmation.

The UV-VIS electronic spectra of supported Fe Schiff base catalysts are shown in **Fig.3.8**. Since Fe(III) (d^5) is a moderately oxidising ion, many of its complexes exhibit ligand to metal charge transfer transitions(LMCT). In general, transitions to both $L \rightarrow e_g$, $L \rightarrow t_{2g}$ levels may be expected [18]. A moderate intensity band at 380nm and a very low intensity band at 490nm are observed in all our catalysts which are atttibuted to the spin - forbidden absorption bands. These assignments are well within the range reported for other Fe(III) complexes of pyridyl and other nitrogen containing ligands[18,19]

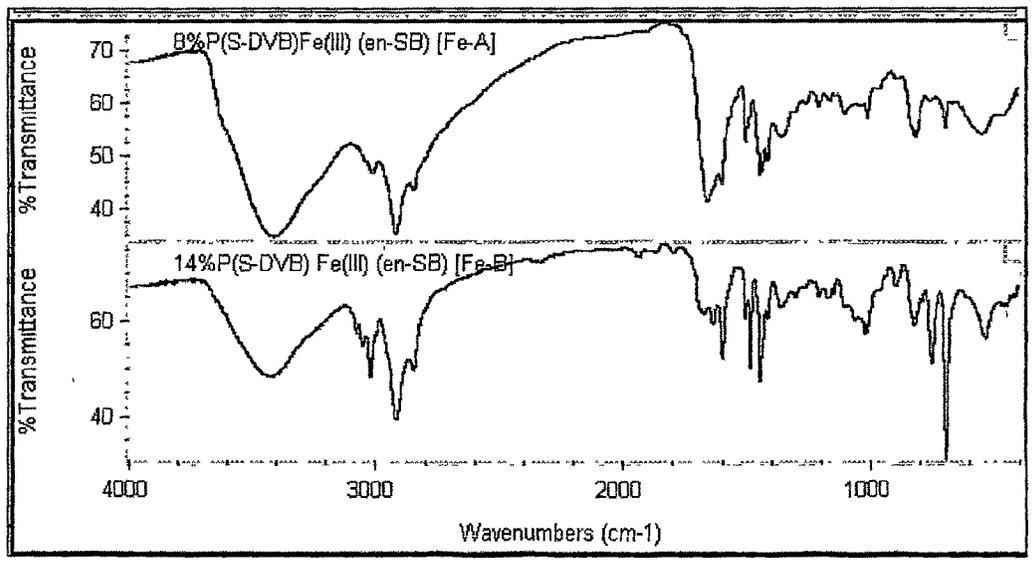

Fig. 3.7 a : I.R. spectra of 8% and 14% P(S-DVB) Fe (III) (en-SB) [Fe-A and Fe- B]

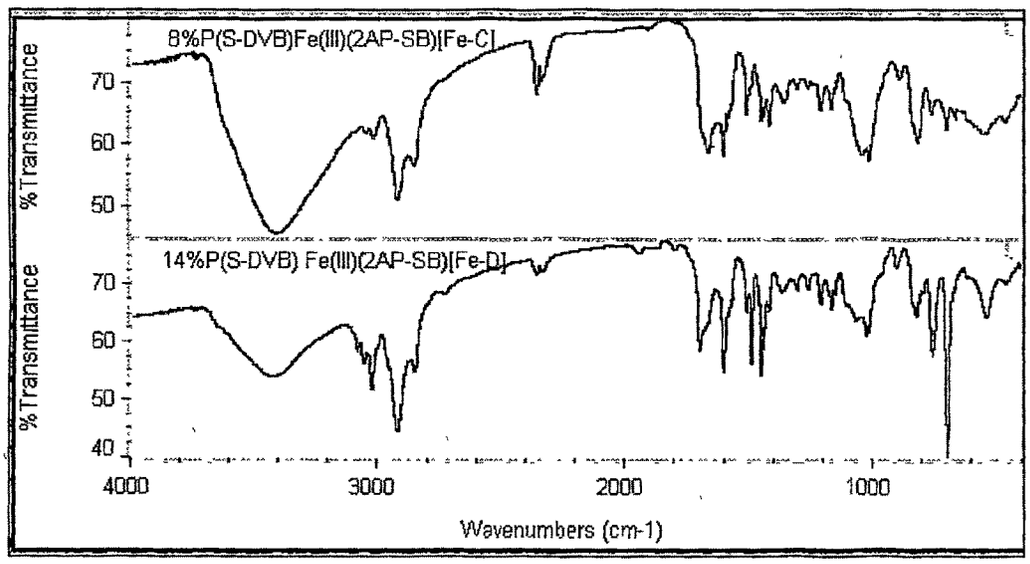

Fig. 3.7 b : I.R. spectra of 8% and 14% P(S-DVB) Fe (III) (2ap-SB) [Fe-C and Fe- D]

Table 3.11
Important i.r.bands (in cm^{-1}) of P(S-DVB)-Schiff base and the supported catalysts

Compound	νN-H	νC=N	Py-ring	Py-ring'N' +νC=N stretch	νFe-Cl	νFe-N
8%P(S-DVB)-(en-SB)	3410ms	1672s				
14%P(S-DVB)-(en-SB)	3430ms	1679s				
8%P(S-DVB)-(2ap-SB)	3415ms	1699s	1454ms 1507ms	777ms		
14%P(S-DVB)-(2ap-SB)	3420ms	1699s	1454ms 1493ms	764ms		
Fe-A	3403ms	1659s			383w	310w
Fe-B	3423ms	1646s			385w	316w
Fe-C	3403ms	1666s	1454ms 1513ms	764ms	386w	316w
Fe-D	3413ms	1676s	1493ms 1413ms	758ms	385w	316w

s - sharp, ms-medium sharp, w-weak

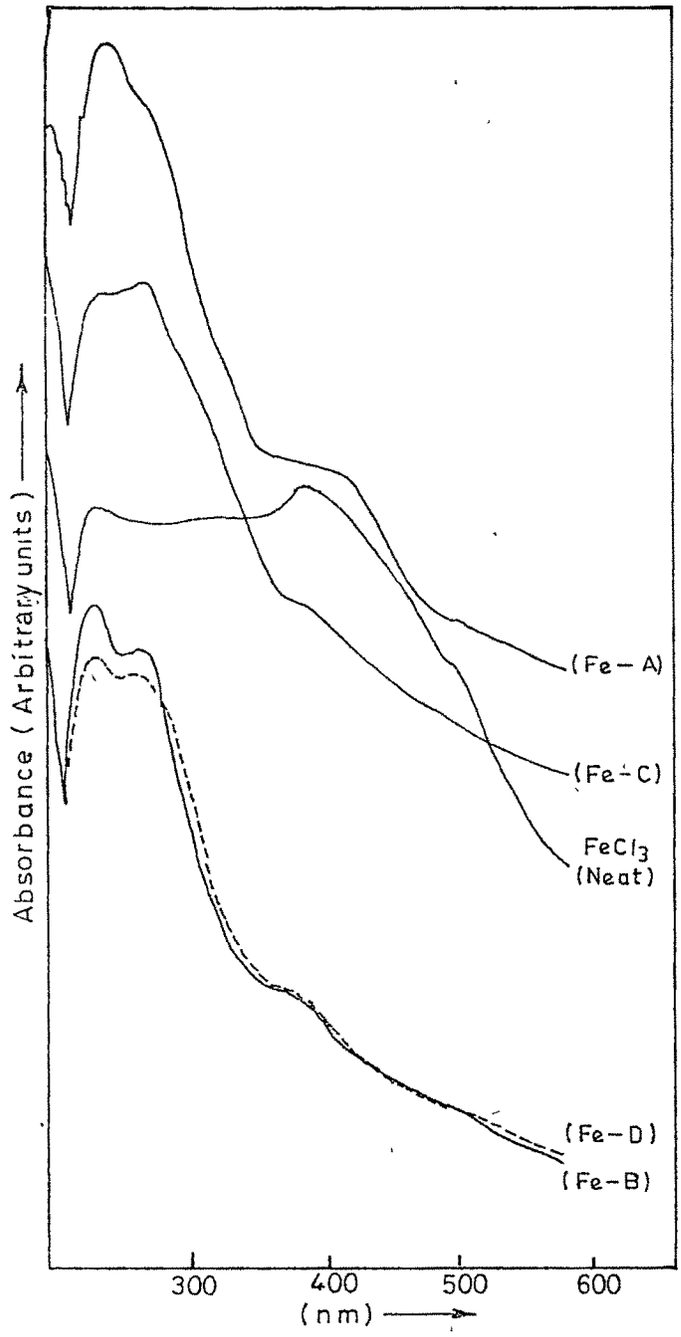

Fig 3 .8 : UV-VIS spectra of Fe(III)-Schiff base complexes

Scanning electron micrograph (SEM) at various stages of preparation of the catalysts were recorded to understand morphological changes occurring on the surface of the polymeric matrix. Initial examination of the SEM's reveal that the Fe(III) atoms are finely distributed across the smooth spherical surface of the beads observable at $x10^4$ magnification. However, accurate analysis regarding the change in distribution profile of Fe on the surface of the matrix before and after the catalytic cycle could not be made due to very low loadings ($\sim 10^{-5}$ mol g^{-1}) of the metal on the support. A representative micrograph is shown in **Plate 3.2.** Similarly in the photoelectron spectra the Fe peaks in the region (712-714 eV) were obscured by intense background spectrum (probably arising due to high carbon content in the polymer). Thus definite conclusions about the oxidation state of Fe in the fresh and spent catalysts could not be made. Again low concentration of Fe was found to limit surface characterization [20].

Thermogravimetric analysis of Fe supported catalysts reveal that they are not stable above 300°C. The TG profile (**Fig.3.9**) indicate that the unsupported polymers degrade at higher temperatures which is also accompanied by higher weight loss (**Table 3.12**). The weight loss observed above 400°C in all the catalysts may be due to the dissociation of attached ligand moieties as well as scission of polymeric chain.

Catalytic Epoxidation

Catalysts **Fe- A - Fe- D** were employed in the oxidation of electron rich olefins such as *cis*-cyclooctene and styrene. These results are compiled in **Table 3.13** and **Table 3.14.** In presence of TBHP all the catalysts effect the epoxidation at room temperature with generally low yield of products (1.4-2.8% of cyclooctene oxide and 6.9-17.3% combined yield of styrene oxide + benzaldehyde). However, at slightly elevated temperature (50°C) there is a marked increase in the corresponding yields of epoxides (7.4 - 23.2% of cyclooctene oxide

a

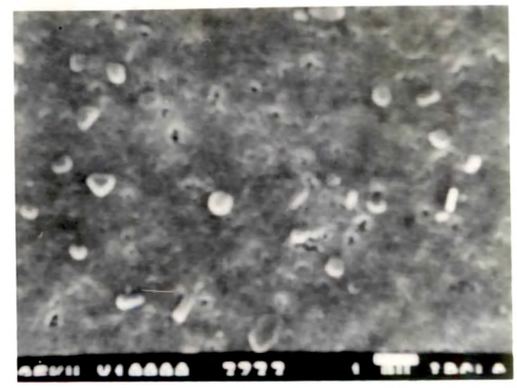

b

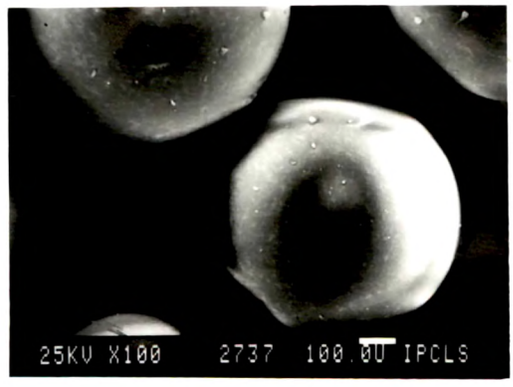

c

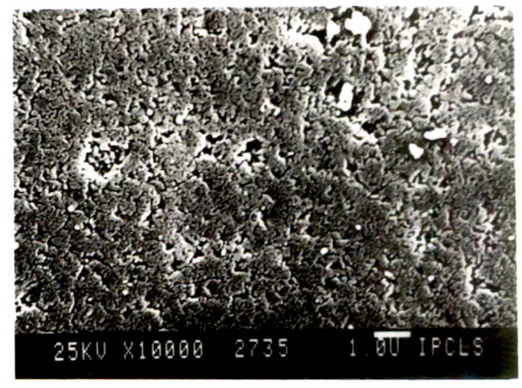

d

Plate 3.2 : Scanning electron micrographs of (a) Fe-A (b) Fe-B (c) Fe-C (d) Fe-D

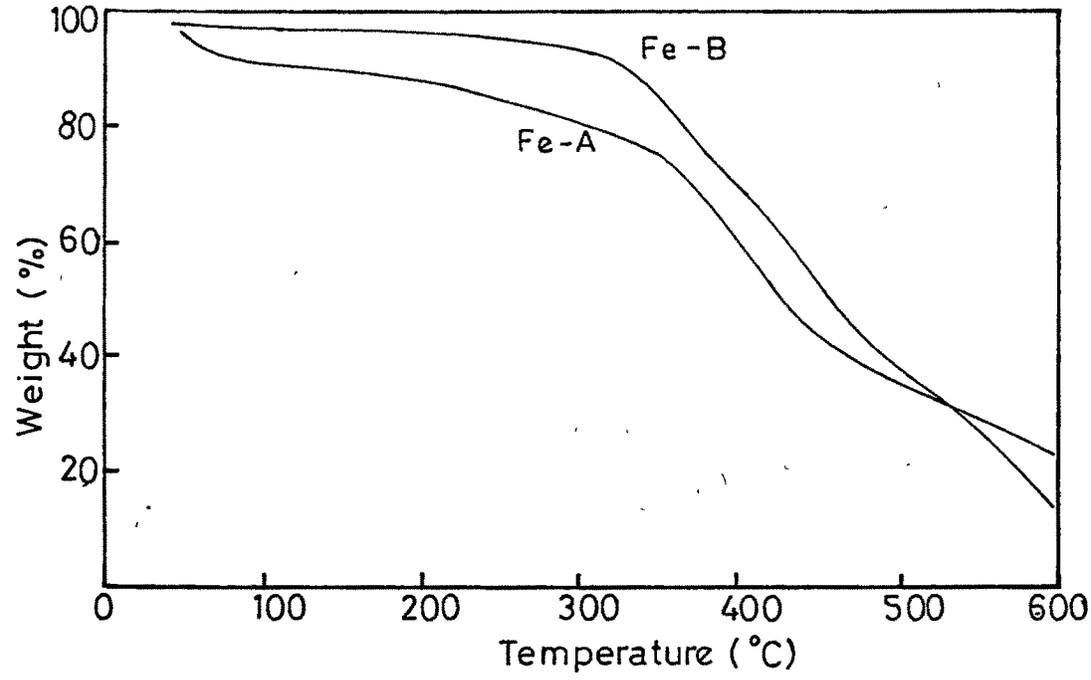

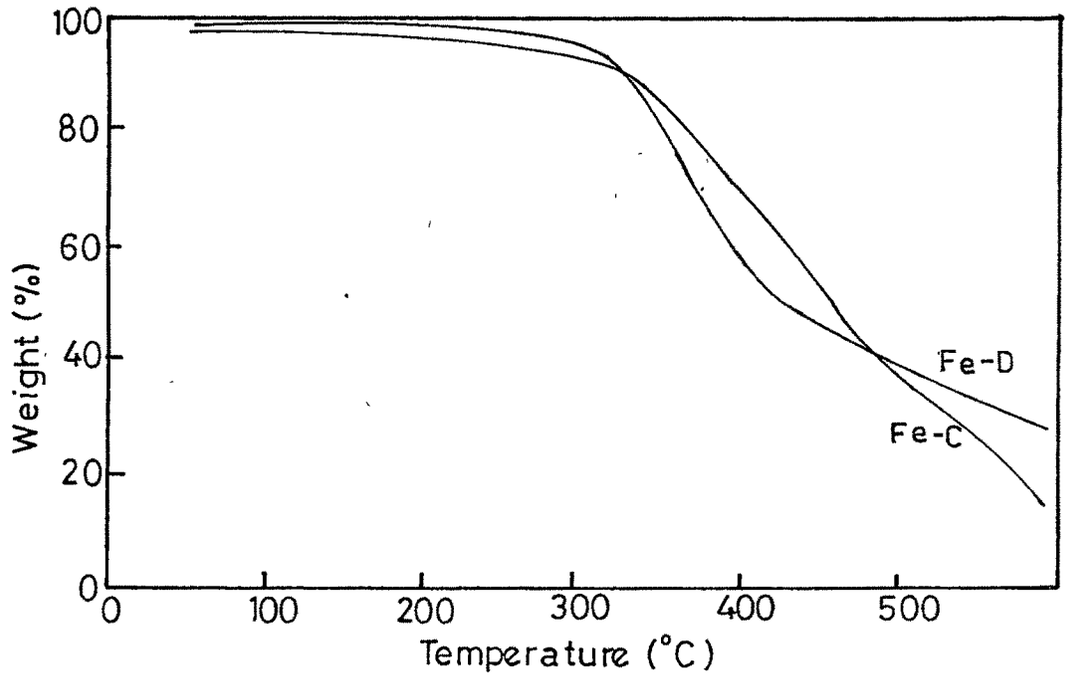

Fig. 3.9. Thermograms of polymer supported Fe(III)-Schiff base complexes

Table 3.12
Thermal data of polymer supported Fe(III)-Schiff base complexes

Ligand/Catalyst	Degradation temp(°C)	Weight loss (%)
8%P(S-DVB)-(en-SB)	412.9	47.2
Fe-A	363 425	27.0 55.0
14%P(S-DVB)-(en-SB)	394.4	61.1
Fe-B	356.5 444.5	15.0 40.0
8%P(S-DVB)-(2ap-SB)	545.5 378.9	57.0 32.7
Fe-C	368 436	30.0 65.0
14%P(S-DVB)-(2ap-SB)	408.9	73.8
Fe-D	379.3 500.5	25.0 79.0

and 38.1- 79.6% combined yields of styrene oxide + benzaldehyde). This observation is evident for both cyclooctene and styrene. Catalytic activity is much more pronounced in acetonitrile medium than in methanol. Interestingly, with *cis*-cyclooctene GC analysis showed the selective formation of cyclooctene oxide. On the other hand in the reaction with styrene, the major product obtained was the secondary oxidation product benzaldehyde (8 - 68.3%) while the epoxide yield was much less (0.9 - 11.3%). The predominant formation of aldehyde indicates that the reaction with the peroxide proceeds beyond the epoxide stage resulting in the oxidative cleavage of styrene. Both **Fe-B** and **Fe-D** showed higher activity than **Fe-A** or **Fe-C** catalysts. Schiff base complexes of other metal ions such as Mn(II), Ni(II) and Cu(II) anchored on to solid supports such as zeolites, clay and macroporous polymer are reported to catalyze olefin epoxidation using iodosylbenzene as the oxygen source[20 - 23]. The catalytic behavior and the selectivity of the end products obtained with the present Fe complexes are comparable and in some cases better results were obtained than that reported for other metal complexes. For a proper understanding of the catalytic efficiency of supported *vis-a-vis* unsupported homogenous Fe-Schiff base complexes, direct comparison of activities under optimized conditions is desirable. Presently, to our knowledge, systematic data on the activity of homogeneous Fe-Schiff base catalysts is not available. The slower rate of reaction(~24h) exhibited by the polymer bound catalysts described above is attributed mainly to the slower diffusion of substrate olefins into the polymer matrix where the active sites are located[24].

Table 3.13
Epoxidation of *cis*-cyclooctene with polymer supported Fe-catalysts[a]

Catalyst	Solvent	Temp(°C)	Cyclooctene oxide (%)[b]
Fe-A	acetonitrile	25	2.8
	methanol	25	1.9
	acetonitrile	50	10.4
	methanol	50	7.4
Fe-B	acetonitrile	25	2.5
	methanol	25	2.6
	acetonitrile	50	20.8
	methanol	50	12.6
Fe-C	acetonitrile	25	2.5
	methanol	25	1.4
	acetonitrile	50	17.3
	methanol	50	13.3
Fe-D	acetonitrile	25	2.8
	methanol	25	2.2
	acetonitrile	50	23.3
	methanol	50	14.2

[a]*Reaction conditions : 250mg of catalyst, 10mmol substrate, 4.25mmol TBHP, 20ml solvent, 24hrs.*
[b]*yield based on oxidant taken*

Table 3.14
Styrene epoxidation with polymer supported Fe catalysts[a]

Catalyst	Solvent	Temp(°C)	Styrene oxide(%)[b]	Benzaldehyde(%)[b]
Fe-A	acetonitrile	25	1.7	8.0
	methanol	25	1.0	7.2
	acetonitrile	50	6.6	57.2
	methanol	50	2.1	36.0
Fe-B	acetonitrile	25	1.2	9.9
	methanol	25	0.9	7.3
	acetonitrile	50	7.2	64.3
	methanol	50	3.4	48.8
Fe-C	acetonitrile	25	0.9	10.0
	methanol	25	0.6	6.2
	acetonitrile	50	10.7	59.0
	methanol	50	5.1	37.0
Fe-D	acetonitrile	25	0.8	16.4
	methanol	25	1.3	13.3
	acetonitrile	50	11.3	68.3
	methanol	50	5.9	52.6

[a]*Reaction conditions 250mg of catalyst, 10mmol substrate, 4.25mmol TBHP, 20ml solvent 24hrs,*
[b]*yield based on oxidant taken*

III. POLY(STYRENE-DIVINYLBENZENE) SUPPORTED 2-AMINOPYRIDINE COMPLEXES

The loading of ruthenium on to the crosslinked poly(styrene-divinylbenzene)-2-aminopyridyl ligand was carried out as per the steps summarized in **Scheme 3.3**. The two polymer anchored metal complexes used in this work for catalytic oxidation of olefins are designated as under:

Ru - E : 8% Poly(S-DVB)-2AP Ru(III)

Ru - F : 14% Poly(S-DVB)-2AP Ru(III)

Both **Ru-E** and **Ru-F** have been characterised by chemical analysis and some of their important physical properties measured. This data is compiled in **Tables 3.15** and **3.16**. Catalyst **Ru-F** has a slightly higher surface area than **Ru-E** and larger pore volume. The higher surface area and pore volume exhibited by **Ru-F** has also resulted in higher loading of the metal on to the polymeric support (**Table 3.16**). Better swelling properties were observed in polar solvents for **Ru-F** than for **Ru-E** (**Table 3.17**). The non-polar solvents like n-heptane and benzene showed much lower percentage swelling for either catalysts.

The i.r. spectra of polymeric ligands and their $RuCl_3$ complexes were recorded separately in the mid i.r (4000-400 cm^{-1}) and the far i.r (500-50 cm^{-1}) regions to ascertain the nature of linkage to the metal. In the 3100-3500cm^{-1} region all compounds exhibited medium to broad intensity bands assigned to the NH stretch as well as the CH stretching mode of the pyridine[14]. On complexation these bands did not show appreciable variation in peak positions. However, there was considerable broadening of the band. Pyridyl ring breathing vibrations are observed as strong bands in the 1600-1400 cm^{-1} region. Slight high frequency shifts in these bands suggests possible co-ordination through the nitrogen of pyridine ring. A strong band due to *sec*-amine(NH) stretching vibration appears in the 1650-1660 cm^{-1} region

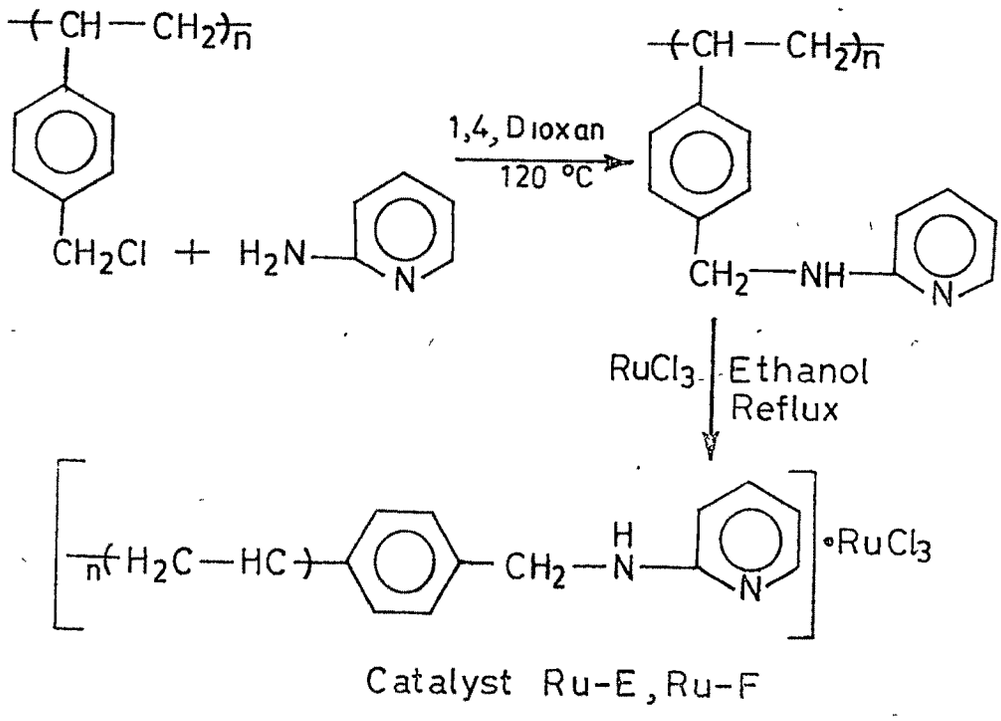

Scheme 3.3 : Synthesis of polymer supported Ru(III)-2-aminopyridine complexes

Table 3.15
Elemental Analysis of Polymer Support, Ligand and Ru-anchored catalysts

Compound	C%	H%	Cl%	N%	Ru (mmol/g resin)
8%P(S-DVB)CH_2Cl	67.61	5.67	22.32	--	--
14%P(S-DVB)CH_2Cl	78.76	7.03	14.21	--	--
8%P(S-DVB)-2AP	66.91	6.11	--	9.13	--
14%P(S-DVB)-2AP	73.41	6.75	--	5.52	--
Ru-E	66.05	6.34	--	9.41	1.4×10^{-5}
Ru-F	75.75	6.80	--	5.10	1.8×10^{-5}

Table 3.16.
Physical properties of Ru-supported P(S-DVB) catalysts

Compound	Surface Area (m^2/g)	Moisture content (wt%)	Bulk Density (g/cm^3)	Pore volume (cm^3/g)
8%P(S-DVB)CH_2Cl	39.1	--	--	--
14%P(S-DVB)CH_2Cl	46.3	--	--	--
Ru-E	31.6	2.54	0.475	0.099
Ru-F	39.4	2.62	0.430	0.196

Table 3.17
Swelling data of Ru-E and Ru-F in different solvents (mol %)

Solvent	Ru-E	Ru-F
Water	5.08	5.27
Methanol	2.80	4.42
Ethanol	1.98	2.10
Acetonitrile	2.20	2.35
Benzene	1.20	1.25
Tetrahydrofuran	1.12	1.19
n-Heptane	0.91	1.06

(**Fig.3.10a,3.10b**). More conclusive information on the coordination of the ligand to the central metal ion comes from the far i.r. data. Low intensity bands due to νM-N and νM-Cl in case of complexes were observed in the 370-450 cm^{-1} region. These observations indicate that the ligand is coordinated to the Ru(III) ion through the 'N' of pyridine ring[15].

The reflectance spectra (200-400 nm) of both **Ru-E** and **Ru-F** display nearly identical features with reference to $BaSO_4$ standard (**Fig.3.11**). A weak intensity band at 310nm appears to be due to d-d transitions of Ru^{3+}[16]. Ligand-metal charge transfer bands were not seen in this region.

The loading of ruthenium on to the surface of the polymeric support was independently examined in the scanning electron micrographs (SEM) of the catalysts and by comparison with the SEM of the parent ligand. At a resolution of 10^4 changes in the morphology of the supported catalysts was clearly noticeable. The dispersion of the metal on the smooth spherical surface is very fine (**Plate 3.3**). A major reason affecting accurate morphological studies is the very low level of metal loading on the polymer matrix, which was generally in the range of 1.4-1.8 x 10^{-3} mmol g^{-1} resin in our system.

Thermogravimetric analysis (TGA) of chloromethylated poly(S-DVB) indicate a single step degradation in the 430-450°C temperature range. Both catalysts **Ru-E** and **Ru-F** on the otherhand degrade at slightly lower temperatures (392-417°C). However, in these catalysts, an additional peak around 250°C with a weight loss of about 25% is clearly noticed. Such a degradation profile was not seen in the starting polymer. It is possible that either the 2-aminopyridyl moiety or the chlorides might dissociate at this temperature from the catalyst surface. Representative thermograms are depicted in **Fig . 3.12.**

3.2 Catalytic Activity

In the presence of mono- oxygen source such as cumene hydroperoxide or iodosylbenzene homogeneous Ru(II) and Ru(III) complexes of diphosphines and tetradentate

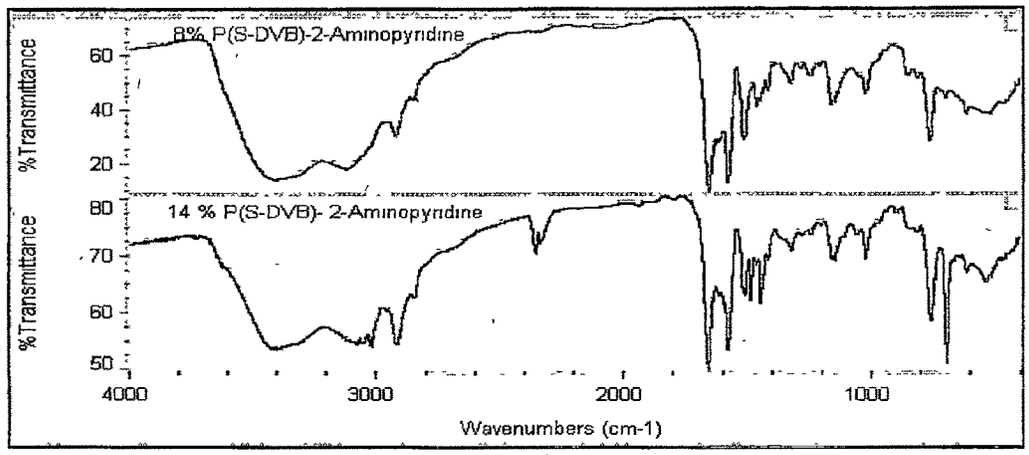

Fig.3.10 a : I.R. spectra of 8% and 14% P(S-DVB)-2 aminopyridine

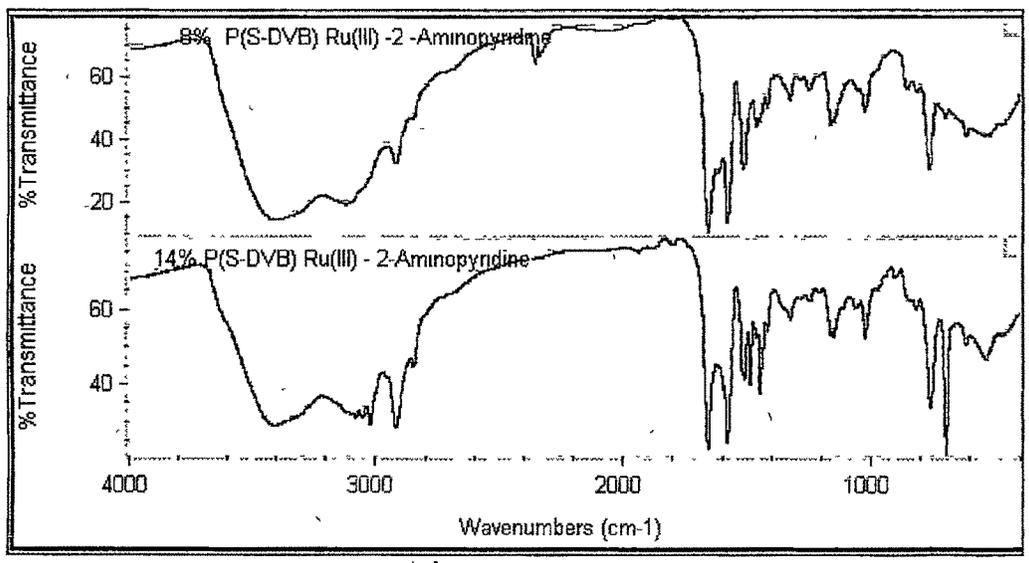

Fig.3.10 b : I.R. spectra of 8% P(S-DVB)- 2 ap Ru(III) [Ru-E] and 14% P(S-DVB)- 2 ap Ru(III) [Ru-F]

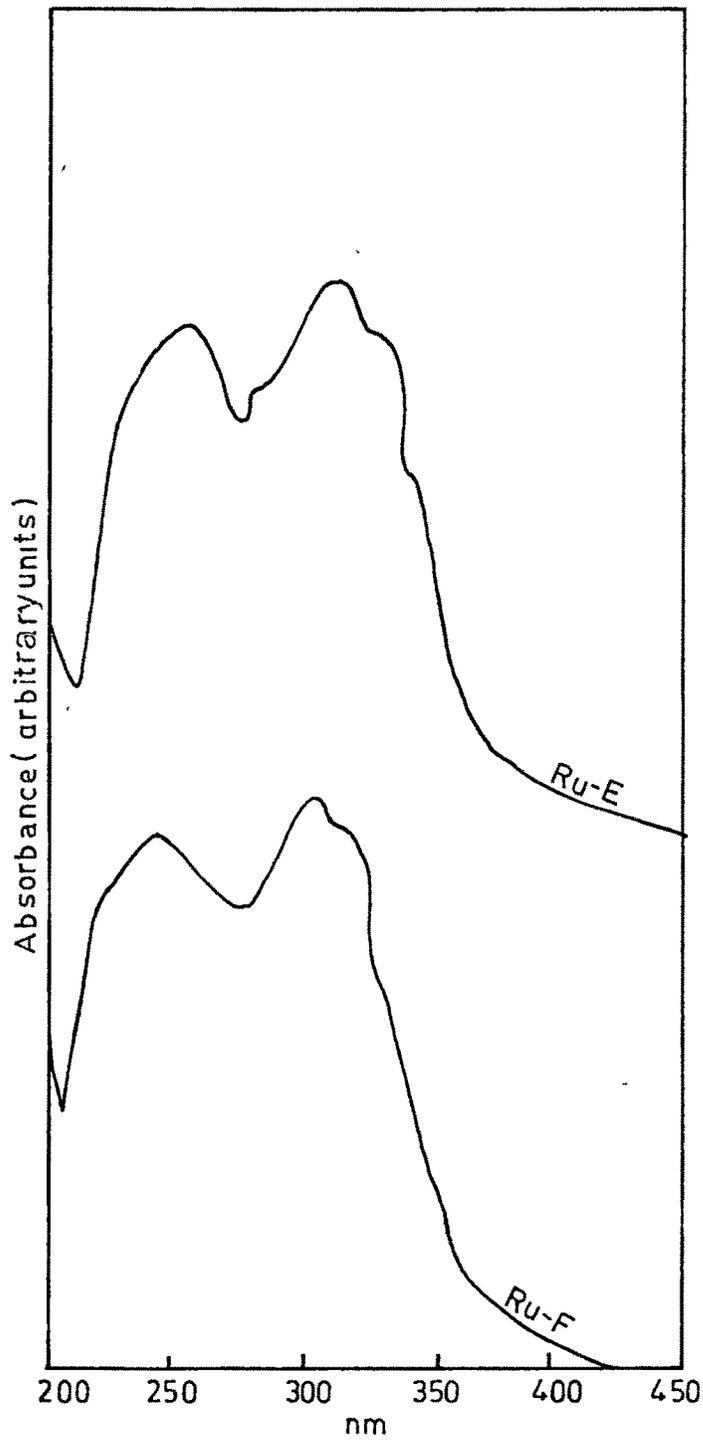

Fig. 3.11 : UV-VIS spectra of Ru(III)-2-aminopyridine complexes

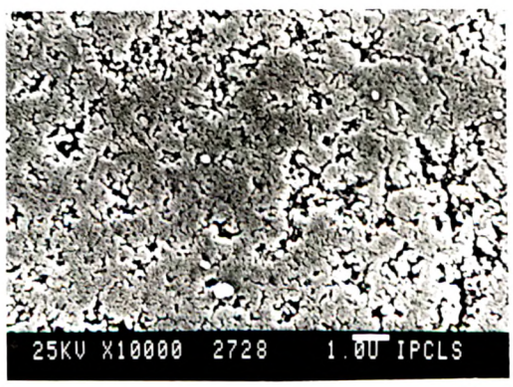

a **b**

Plate 3.3 : Scanning electron micrographs of (a) Ru-E (b) Ru-F

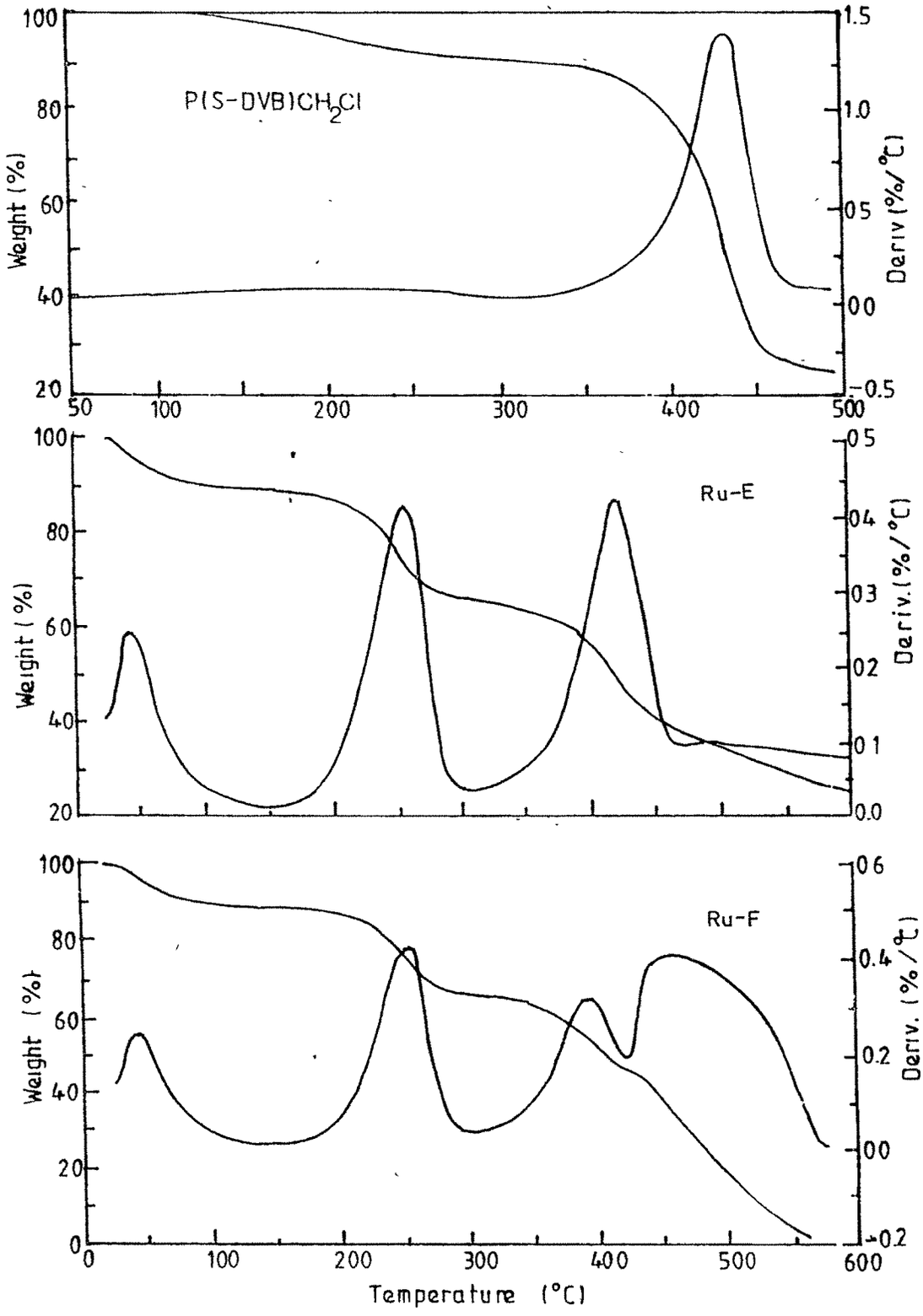

Fig.3.12. Thermal analysis of chloromethylated P (S-DVB), Ru-E and Ru-F

Table 3.18
Thermoanalytical data of P (S-DVB) and ruthenium anchored catalysts

Compound	Temp.(°C)	Wt. loss (%)
8%P(S-DVB)CH_2Cl	453.3	71.0
14%P (S-DVB)CH_2Cl	432.9	35.6
Ru-E	254.7 417.7	26.4 50.1
Ru-F	254.1 392.6	25.6 47.8

Schiff bases are known to catalyze the epoxidation of alkenes in the liquid phase[17,18]. Using the Ru-anchored catalysts **E** and **F** different olefins were subjected to epoxidation. The results of room temperature epoxidation of *cis*-cyclooctene, styrene and cyclohexene by **Ru-E** and **Ru-F** are compiled in **Tables 3.19** to **3.21**. Initially an induction period of about 30-40min was observed for both **Ru-E** and **Ru-F.** Moreover, comparable olefin conversions could be reached only after 24hrs reaction time. Such slower rates of catalysis has often been encountered by other workers using transitional metal complexes bound to surfaces of functionalised polymers[19,20]. This behaviour is primarily due to the slow diffusion of substrate olefins from the solution phase to the active metal centres in the polymer matrix leading to the rate limiting process. In the present case despite the relatively poor swellability of the macroporous polymer bound metal complexes (<6 %) in common organic solvents, the overall good conversions to epoxides (upto 82 %) indicates that catalytic sites are essentially localized in the accessible regions of the polymer matrices.

In the case of *cis*-cyclooctene the corresponding epoxide was formed. The yield increases significantly from 9 to 50 % when the temperature was increased from 25°C to 50°C as shown in **Table 3.19.** With $RuCl_3$ alone (prior to the anchoring on the polymer) the epoxide formed was only 3% (at 25°C). Interestingly, with styrene as substrate the epoxide was a minor product (yield 14%) whereas the secondary oxidation product benzaldehyde was found to be the major product(80%). Both catalysts showed better reactivity in acetonitrile compared to methanol. Once again the yields were much higher at 50°C than at 25°C (**Table 3.20**). Finally, the oxidation of cyclohexene gave multiple products namely cyclohexene oxide, 2-cyclohexene-1-ol and 2-cyclohexene-1-one (**Table 3.21**). Yields of 1-one was much higher than the epoxide or 1-ol. In general, **Ru-F** showed marginally better catalytic activity than **Ru-E.**

Table 3.19
Epoxidation of *cis*-cyclooctene

Catalyst	Solvent	Temp.(°C)	Epoxide (%)[a]
Ru-E	CH_3OH	25	9.1
	CH_3OH	50	27.7
	CH_3CN	25	11.4
	CH_3CN	50	50.7
Ru-F	CH_3OH	25	8.4
	CH_3OH	50	27.2
	CH_3CN	25	12.2
	CH_3CN	50	45.1
No catalyst	CH_3OH	25	traces
	CH_3CN	25	no reaction

Weight of catalyst=0.25 g ; Substrate = 10 mmol ; TBHP = 4.25 mmol, Time = 24 hrs ; Solvent = 20mL
[a]*yield based on oxidant taken*

Table 3.20
Epoxidation of styrene by P (S-DVB)-2AP Ru (III)catalysts

Catalyst	Solvent	Temp. (°C)	Product yield (%)[a]	
			Styrene oxide	Benzaldehyde
Ru-E	CH_3OH	25	0.6	2.4
	CH_3OH	50	3.5	22.4
	CH_3CN	25	3.3	47.6
	CH_3CN	50	13.9	82.2
Ru-F	CH_3OH	25	0.5	8.2
	CH_3OH	50	4.0	35.9
	CH_3CN	25	2.6	38.9
	CH_3CN	50	16.9	79.3
No catalyst	CH_3OH	25	--	0.65

Weight of Catalyst=0.25 g , Substrate = 10 mmol ; Solvent = 20 ml , TBHP = 4 25 mmol , Time = 24 hrs
[a] *yield based on oxidant taken*

Table 3.21
Cyclohexene epoxidation by P(S-DVB)-2AP Ru (III) catalysts

Catalysts	Solvent	Temp (°C)	Product Yield (%)[a]		
			Epoxide	2-cyclohexene-1-ol	2-cyclohexene-1-one
Ru-E	CH_3OH	25	1.0	1.3	6.1
	CH_3OH	50	0.9	5.1	41.7
	CH_3CN	25	0.4	0.1	18.4
	CH_3CN	50	2.2	1.7	64.4
Ru-F	CH_3OH	25	0.5	0.6	14.5
	CH_3OH	50	1.7	8.7	50.9
	CH_3CN	25	0.3	1.9	18.9
	CH_3CN	50	2.4	1.2	64.9
No catalyst	CH_3OH	25	--	--	No reaction

Weight of Catalyst = 0.25 g, Solvent = 20 ml, Cyclohexene = 10 mmol,TBHP = 4.25 mmol , Time = 24 hrs
[a]*yield based on oxidant taken*

In order to understand the effect of various reaction parameters on catalytic performance a systematic study was carried out on the oxidation of *cis*-cyclooctene as the substrate using **Ru-E** as the catalyst. The extent of epoxidation observed at different temperatures and catalyst concentrations is summarized in **Table 3.22**. From the results obtained it is clear that both temperature and the initial amount of catalyst influence the oxidation reaction much more than the absolute volume (quantity) of the substrate olefin. A plot of cyclooctene conversion *vs.* reaction time at 50°C indicates that under a fixed oxidant concentration both catalyst **Ru-E** and **Ru-F** tend to reach a plateau after 24 hrs (**Fig. 3.13**). with **Ru-F** exhibiting slightly higher conversion.

Table 3.22
Epoxidation of *cis*-cyclooctene by Ru-E under different reaction conditions

	Cyclooctene (mmol)	Catalyst wt. (g)	Temp. (°C)	Epoxide[a] (%)
(a) **Temp. effect**	10	0.25	25	9.0
	10	0.25	40	16.2
	10	0.25	50	26.9
(b) **Catalyst Conc. effect**	10	0.10	50	9.5
	10	0.20	50	12.9
	10	0.25	50	26.9
(c) **Substrate effect**	10	0.25	50	26.9
	30	0.25	50	29.6
	40	0.25	50	34.2

Solvent =CH_3OH, 20 ml ; TBHP = 4.25 mmol ; Reaction time = 24 hrs
[a]yield based on oxidant taken

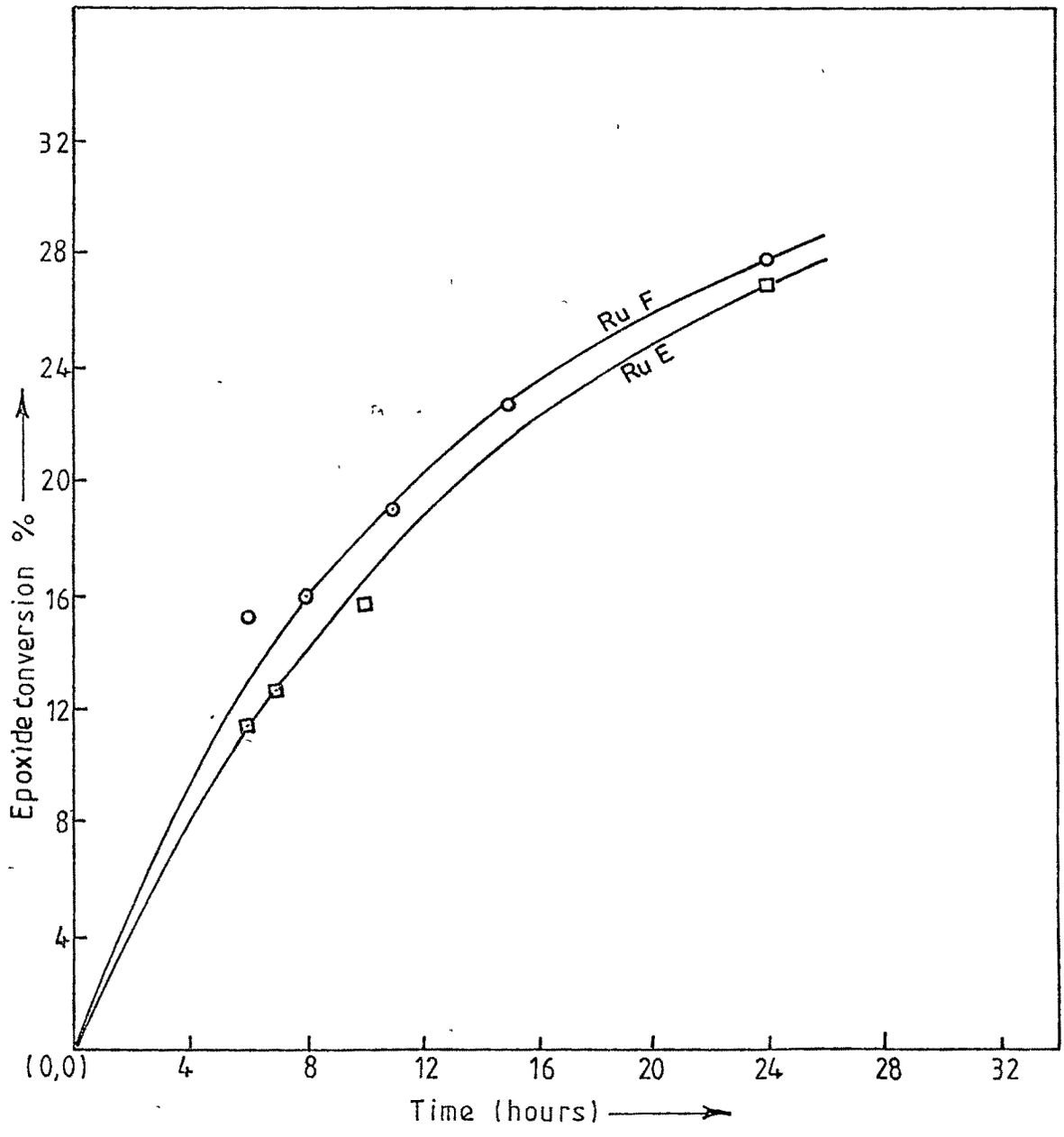

Fig. 3.13 : Profile of conversion *vs* time of catalysts Ru-E and Ru-F

IV. MECHANISTIC ASPECTS

Both homogeneous and heterogeneous catalysts capable of selectively epoxidising a wide range of olefins have been developed. Much progress has been made in understanding the nature of the active catalyst and the mechanism involved in their formation[23-30].

For epoxidation of alkenes using *tert*-butylhydroperoxide, the mechanistic model of Sheldon [31], Gould [32], Imanura et.al [33] and Sherrington et.al [34] has been extended to our system. The reactions of alkyl hydroperoxides in the presence of metal catalysts follow two major pathways [10,35-36]

(a) homolytic and (b) heterolytic

Homolytic decomposition of alkyl hydroperoxides is catalyzed by transition metal complexes and involves *tert*-alkoxy and *tert*-alkylperoxy radicals as reactive intermediates formed *via* the one electron redox processes whereas in heterolytic reactions of alkyl hydroperoxides the principal function of the metal catalyst is to withdraw electrons from the O----O bond *via* coordination, thus making it more susceptible to heterolysis by attacking nucleophiles. The extent of charge transfer is related to the Lewis acidity of the catalysts which generally increase with increasing oxidation state of the central metal atom [16]. Moreover, it has been found that the peroxometal species are generally favoured with early transition metals viz. Mo(VI), W (VI), V(V) etc.[10]. On the other hand many from transition metals including the ruthenium, iron follow the metal oxo catalyzed route[35].

Experiments were carried out to ascertain the nature of oxidation using 2,6 di-*tert*-butyl 4-methylphenol (BHT) as a free radical trap which is known to scavenge the peroxy radicals produced by homolytic scission of peroxidebond[38]. Carbontetrachloride(CCl_4)was used to find out whether there is an involvement of free radicals in the reaction[39].

The experimental procedure adopted to study the probable mechanistic pathway is as follows :

250mg of polymer supported metal complex was placed in a 2-necked round bottomed flask containing 20ml methanol. The catalyst beads were allowed to swell in the solvent for about 30mins. To this, BHT (0.2mmole) was added, followed by slow addition of *cis*-cyclooctene (10mmole). After a brief agitation, TBHP (70% in H_2O, 4.25mmole) was quickly added using a graduated pipette. The solution was stirred for 24hrs at 50°C. the extent of product formation was estimated by GC analysis using chlorobenzene as internal standard.

In another experiment to test the involvement of free radicals, CCl_4 (0.2 mmole) was added to the reaction mixture prior to the addition of TBHP. The results of these studies on representative catalysts are given in **Table 3.23.**

It is known that BHT scavenges peroxy free radicals suppressing the yield of epoxide by radical autooxidation (homolytic cleavage of peroxide bond) process. Results indicate that BHT did not completely suppress the reaction but the epoxide yields were reduced. The overall reduction in yields was 22-24 % for ruthenium catalyst and about 32-40% for iron catalysts. Similarly, in experiments with CCl_4 considerable lowering in epoxide yields was observed. In both these experiments the reaction is only partially suppressed and no other free radical induced side products were detected. By-products result from subsequent reactions of alkoxy and alkylperoxy radicals with the substrate[40]. For the present Ru(III) and Fe(III) catalysts preliminary results suggests that the major route for epoxide formation is by a heterolytic mechanism. However, simultaneous existence of a homolytic reaction cannot be overruled. A simplified dual mechanistic pathway for the catalytic epoxidation of *cis*-cyclooctene by Fe(III) catalysts in presence of TBHP is shown in **Scheme 3.4** which can be extended to Ru(III) systems. It may be pointed out that the involvement of active oxo-Ru(V)

Table 3.23
Epoxidation of *cis*-cyclooctene with polymer supported catalyst using additives[a]

Catalyst	Additive	Temp.(°C)	*Cis*-cyclooctene(%)[b]
Ru-A	BHT	25	3.6 (4.9)*
		50	18.2 (23.2)
	CCl_4	50	10.3 (23.2)
Ru-D	BHT	25	13.0 (16.9)
		50	23.2 (30.4)
	CCl_4	50	16.7 (30.4)
Fe-B	BHT	25	1.7 (2.6)
		50	7.5 (12.6)
	CCl_4	50	2.9 (12.6)
Fe-C	BHT	25	0.9 (1.4)
		50	9.0 (13.3)
	CCl_4	50	5.0 (13.3)
Ru-F	BHT	25	5.3 (8.4)
		50	20.7 (27.2)
	CCl_4	25	12.7 (27.2)

[a]*Reaction Conditions . Solvent = methanol (20 ml), cis-cyclooctene =10mmole TBHP = 4.25 mmole , Additive = 0.2mmole*
[b]*yield based on oxidant taken*
**values in the parenthesis indicate the % yield in absence of additive*

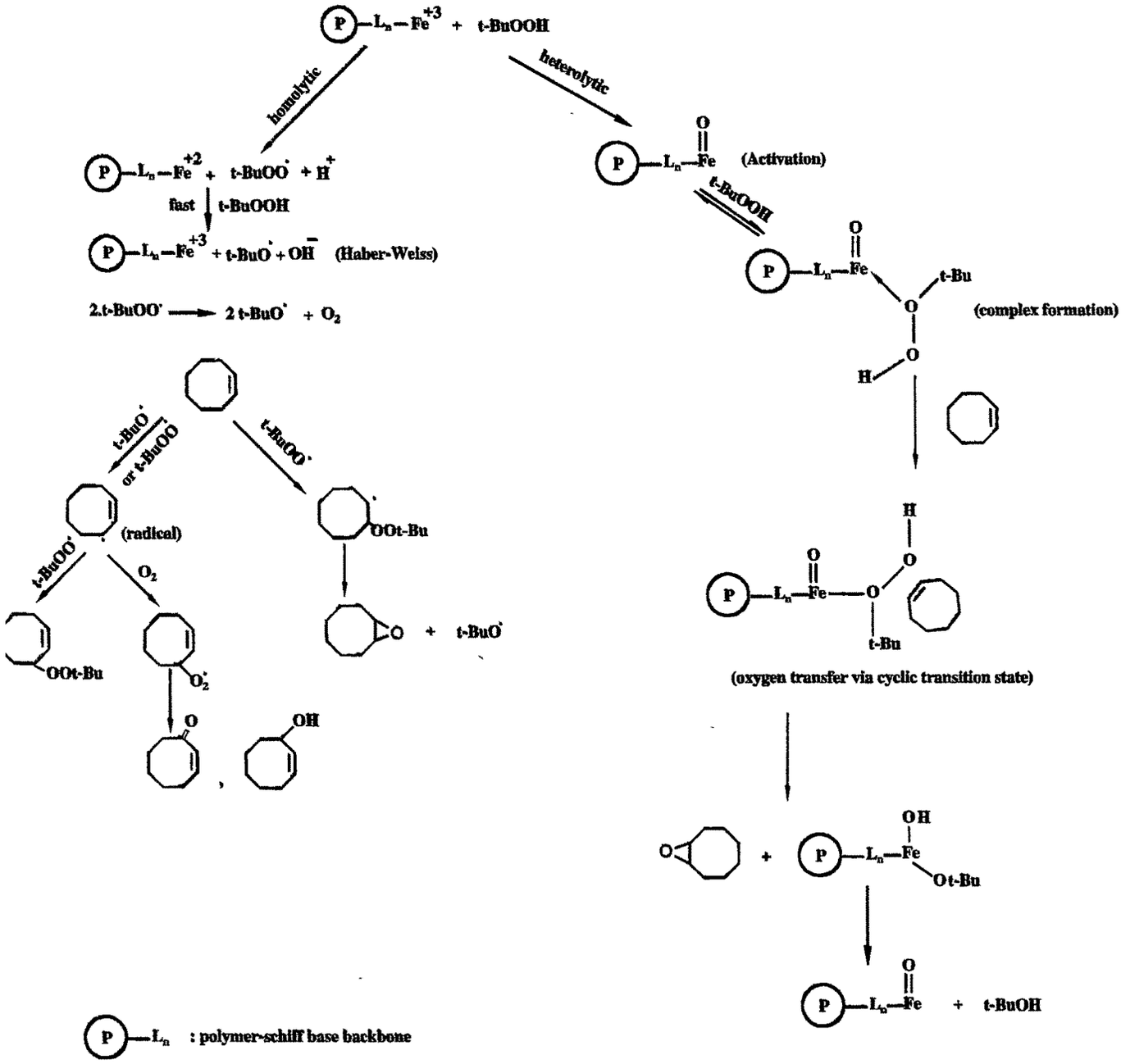

Scheme 3.4 : Probable Mechanistic Pathways for Olefin Epoxidation

and a high valent active complex as shown ((P)- L_n - Fe^{+5} = O) during the epoxidation can be postulated for our system but direct experimental evidence for the formation of these species is lacking .

V. LIFE CYCLE STUDIES

One of the main objectives of supporting a homogeneous metal complex on to a polymer is to enhance the life of the resulting catalyst. To be a truly effective polymer supported catalyst, it is critical that recovery be simple, efficient and that the recovered catalyst retain their activity through multiple cycles[23,24]. A few polymer supported Ru(III) and Fe(III) catalysts were selected to study the extent of recyclability. The results of the experiments carried out are presented in **Table 3.24.**

From **Table 3.24** it can be inferred that the catalysts can be recycled about 5-6 times. However, there is a progressive loss in activity with lowering of epoxide yields. The trend is depicted in **Fig.3.14.** Estimation of ruthenium and iron present in the catalysts after 5-6 cycles revealed a lowering of ruthenium and iron content by 30 - 35%. The slow deactivation of the catalyst is accompanied by a gradual colour change of the catalyst surface with every recycle.

Table 3.24
Recycling studies of catalysts in epoxidation of cis-cyclooctene[a]

Cycle No.	Epoxide(%)[b]				
	Ru-A	**Ru-C**	**Fe-A**	**Fe-C**	**Ru-E**
1	23.2	27.6	7.4	13.3	27.7
2	22.4	26.2	6.9	13.1	18.4
3	21.7	25.1	5.3	12.1	12.7
4	20.4	23.9	4.9	11.7	9.3
5	19.7	21.4	4.8	10.8	3.1
6	12.3	16.1	2.8	6.0	-

[a]*Reaction Condtions : 250mg catalyst, 10mmol cis-cyclooctene, 20 ml methanol, 4.25 mmol TBHP, 50°C , 24hrs.*
[b]*yield based on oxidant taken*

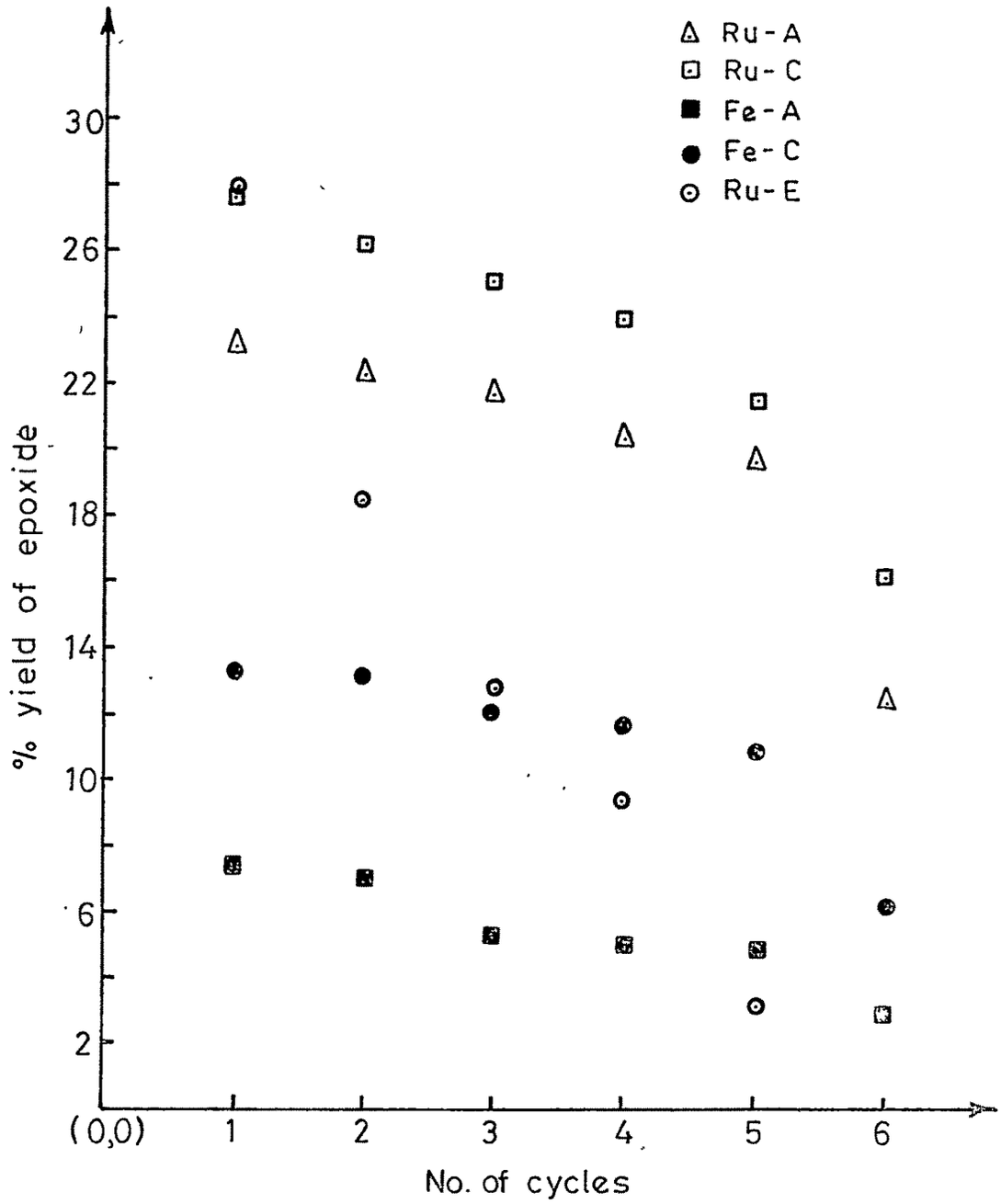

Fig. 3.14 Profile of Catalyst Recycling study

VI. POLY(STYRENE-DIVINYLBENZENE) SUPPORTED PD (II)-SCHIFF BASE COMPLEXES

The functionalisation of the chloromethylated poly(styrene-divinylbenzene) by a Schiff base ligand and the loading of palladium metal to form the polymer supported palladium-Schiff base complex was carried out as shown in **Scheme 3.5**. The catalysts employed in the study are designated as :

Pd-A : 8% Poly(S-DVB) Pd(II) (en-SB)

Pd-B : 14% Poly(S-DVB) Pd(II) (en-SB)

Pd-C : 8% Poly(S-DVB) Pd(II) (2ap-SB)

Pd-D : 14% Poly(S-DVB) Pd(II) (2ap-SB)

Catalyst characterization

Elemental composition of **Pd-A** to **Pd-D** at different stages of preparation are presented in **Table 3.25**. The physical properties of the synthesized catalysts are shown in **Table 3.26**. From the table it can inferred that the nitrogen content in the **Pd-A** and **Pd-C** is higher than in **Pd-B** and **Pd-D** which is attributed to the variation in the degree of crosslinking of the supports. Moreover, less functionalisation is observed in **Pd-B** and **Pd-D**, as in case of supports with higher degree of crosslinking, the polymer network consists of dense and inaccessible domains leading to less functionlisation[41]. A lowering of surface area in the catalysts **Pd-A** to **Pd-D** is observed (**Table3.26**) on loading the metal on to the functionalised polymer support. This indicates that blocking

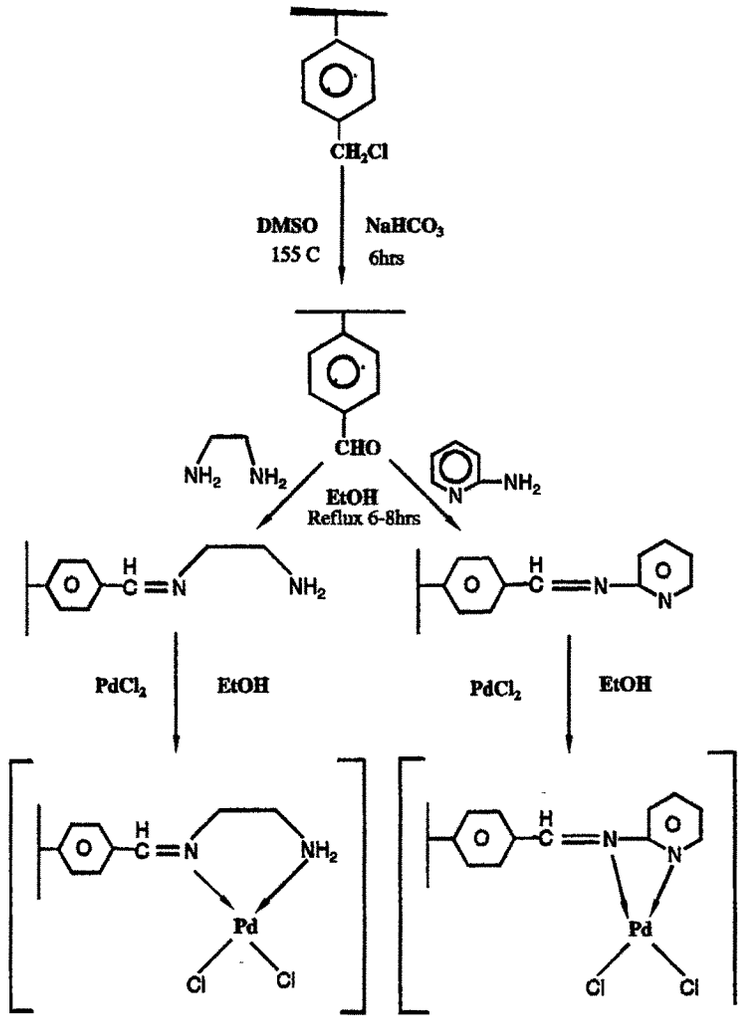

Pd-A and Pd-B **Pd-C and Pd-D**

Scheme 3.5 : Synthesis of polymer supported Pd(II) Schiff base complexes

Table 3.25
Elemental analysis of catalysts at various stages of preparation

Compound	C%	H%	Cl%	N%	Pd mmole/gm of resin
8% P(S-DVB)-CH_2Cl	67.62	5.67	22.32	--	---
14% P(S-DVB)-CH_2Cl	81.79	7.03	14.21		---
8% P(S -DVB) - CHO	81.36	7.03			---
14% P(S -DVB) - CHO	86.20	7.49	-	-	---
8% P(S-DVB)(en-SB)	76.55	7.08	-	2.03	---
14 % P(S-DVB)(en-SB)	85.56	7.63	-	1.66	---
8% P(S-DVB) (2ap-SB)	75.76	6.61	-	1.10	---
14% P(S-DVB) (2ap-SB)	84.65	7.36	-	1.05	---
Pd-A	71.85	6.62	-	1.62	4.32×10^{-5}
Pd-B	82.46	7.48	-	1.44	2.76×10^{-5}
Pd-C	75.56	6.50	-	0.97	4.78×10^{-5}
Pd-D	84.35	7.28	-	0.86	3.03×10^{-5}

of pores of the functionalised polymer support takes place on complexation [42]. **Pd-A** and **Pd-B** have higher surface area (32.7 and 34.16 m^2g^{-1}) than **Pd-C** and **Pd-D** (31.05 and 31.17 m^2g^{-1}) which can be ascribed to the relative size difference of Schiff base derived from ethylenediamine and 2-amino-pyridine [43]. Swelling behaviour of the catalysts in polar and non-polar solvent has been studied (**Table 3.27**). From the swelling data, water, methanol and acetonitrile showed higher percentage of swelling. However, for practical purposes, methanol was used as a solvent of choice as it showed a better property for the dissolution of the substrate olefin.

The mid IR (4000 - 400cm^{-1}) and far IR (400 - 200cm^{-1}) spectra of the catalysts at different stages of preparation were recorded (**Fig.3.15**) and the i.r frequencies are compiled in **Table 3.28**. From the i.r data, C=N (azomethine) band in the 1660 cm^{-1} region in Schiff base liganded polymer shifts to lower values (1646 - 1613 cm^{-1}) on complexation with palladium indicating "N" coordination of the ligand to the Pd(II) metal ion. Further, the complexation of ethylenediamine Schiff base to Pd(II) is indicated by a marginal low frequency shift in the ν NH band (~ 3400 cm^{-1}) in case of **Pd-A** and **Pd-B**. Similarly the coordination of 2-aminopyridine Schiff base to Pd (II) in **Pd-C** and **Pd-D** is confirmed by a shift to lower values (from 1606 cm^{-1} to 1606cm^{-1} and 1568 cm^{-1} to 1513 cm^{-1}) in the pyridine ring frequencies on complexation [44].

The UV-VIS reflectance spectra of the catalysts are shown in **Fig. 3.16**. Due to low metal loading (~10^{-5} mole g^{-1} of resin) the intensities of the bands are affected. Low intensity bands at 240nm and 320nm are observed in all our catalysts, which are assigned

Table 3.26
Physicochemical properties of catalysts

Property	Pd-A	Pd-B	Pd-C	Pd-D
Surface Area(m^2g^{-1})	32.72	34.16	31.05	31.17
Pore Volume (cm^3g^{-1})	0.206	0.207	0.191	0.203
Apparent Bulk Density	0.460	0.465	0.450	0.445
Moisture content (%)	1.50	1.37	1.02	0.98

Table 3.27
Swelling behaviour of catalysts at 25°C (mole%)

SOLVENT	Pd-A	Pd-B	Pd-C	Pd-D
Water	4.32	5.25	4.92	5.66
Methanol	2.62	2.85	2.74	2.95
Ethanol	1.85	2.05	1.98	2.19
Acetonitrile	2.09	2.32	2.21	2.46
Benzene	1.27	1.25	1.22	1.28
THF	1.12	1.18	1.18	1.27
n-Heptane	0.87	0.87	0.92	1.00

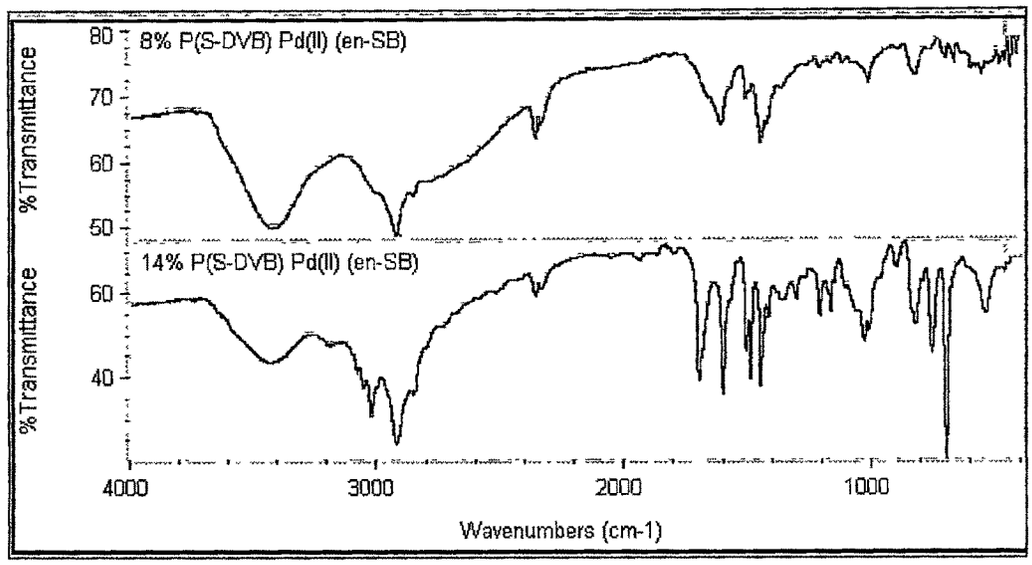

Fig.3.15 a : I.R. spectra of 8% and 14% P(S-DVB) Pd (II) (en-SB) [Pd-A and Pd- B]

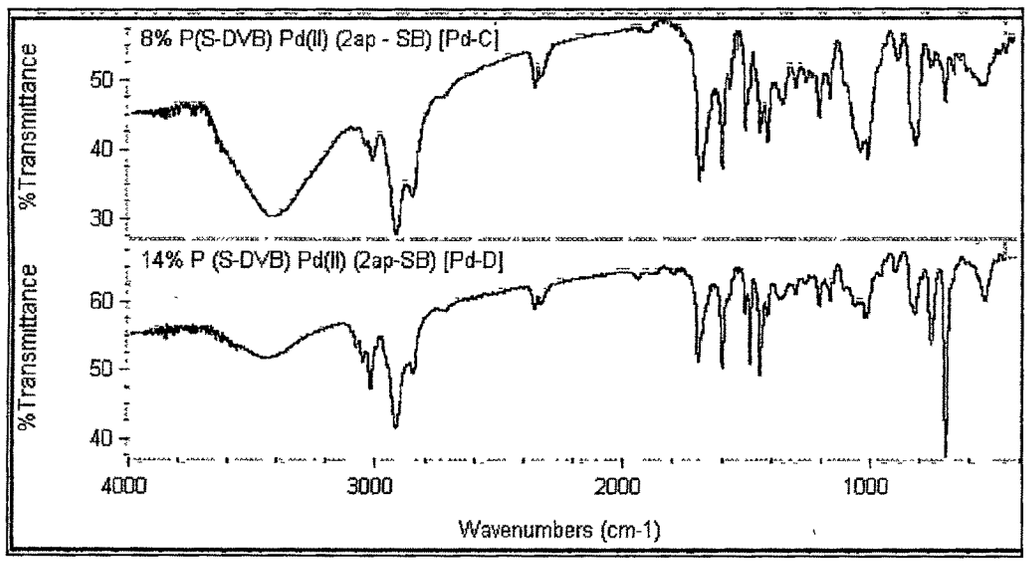

Fig. 3.15b : I.R. spectra of 8% and 14% P(S-DVB) Pd(II) (2ap-SB) [Pd-C and Pd- D]

Table 3.28
I.R. frequencies of poly(styrene-divinylbenzene) supported Schiff base and their palladium complexes

Compound	ν NH	ν C=N	Py-ring	Py-ring'N' + ν C=N stretch	ν Pd-Cl	ν Pd-N
8%P(S-DVB)(en-SB)	3410br	1646s				
14%P(S-DVB)(en-SB)	3430br	1646s				
8%P(S-DVB) (2ap-SB)		1669s	1606ms 1568ms	777ms		
14%P(S-DVB) (2ap-SB)		1669s	1606ms 1568ms	764ms		
Pd-A	3406br	1613s			310w	480w 525w
Pd-B	3423br	1626s			359w	466w 543w
Pd-C		1649s	1600ms 1513ms	758ms	355w	485w 521w
Pd-D		1649s	1600ms 1513ms	754ms	362w	467w 543w

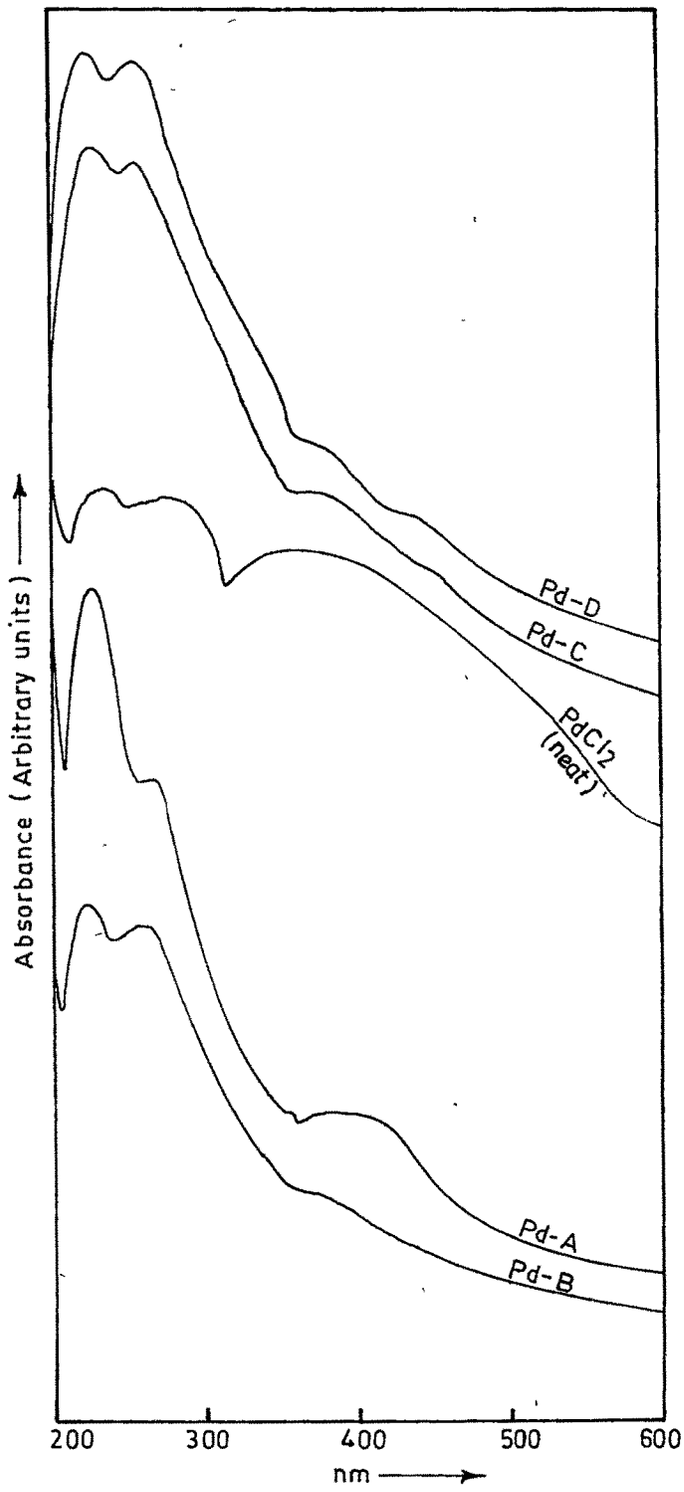

Fig. 3.16. UV-VIS spectra of polymer supported Pd(II)-Schiff base complexes

to $Pd^{+2} \longrightarrow N$ coordination [45,46]. Ligand to metal charge-transfer bands (LMCT) were not seen in this region.

The Scanning electron micrograph (SEM) of the catalysts was recorded in order to understand the morphological changes occurring on the surface of the polymer matrix. At a resolution of $x10^4$ (magnification) there is a fine dispersion of palladium on the smooth spherical surface of the support. More accurate information on the morphological changes on the surface of the polymer matrix could not be obtained due to the very low loading ($\sim 10^{-5}$ mol/g) of palladium on the support. Representative micrographs are shown in **Plate 3.4**.

Thermogravimetric analysis (TGA) of the palladium-supported catalysts indicate degradation in the 400-450°C temperature range (**Table 3.29**). There is an increase in the thermal stability of the polymer supported catalysts with increase in the crosslink of the polymeric support. The degradation of polymer supported metal complexes at lower temperature with higher weight loss may be due to the dissociation of the Schiff base ligand moiety from the catalyst surface.

Hydrogenation of *Cis*-cyclooctene

The kinetics of *cis*-cyclooctene hydrogenation was investigated for catalysts **Pd-A** to **Pd-D**. The data for the hydrogenation reactions were obtained in a kinetic regime as discussed in Chapter 2.

By measuring the hydrogen uptake at different intervals of time for each reaction the rate of hydrogenation was calculated as the slope of the plot of volume of hydrogen absorbed (STP) as a function of time. A representative plot is shown in **Fig. 3.17**. The results are

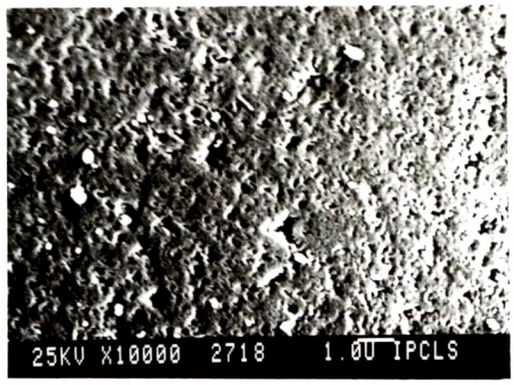

a

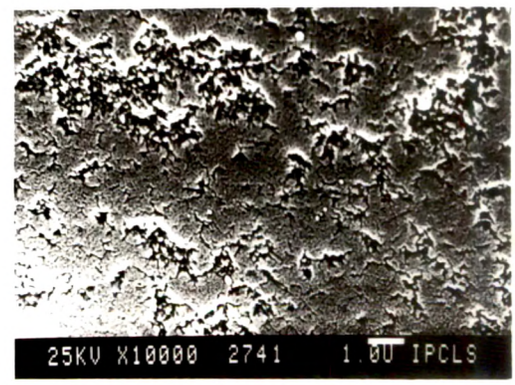

b

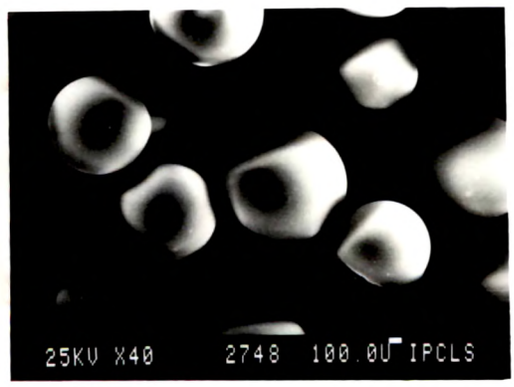

c

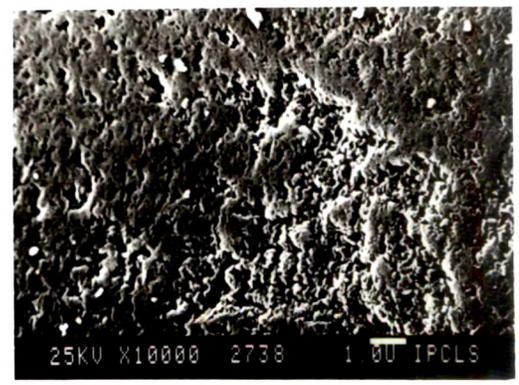

d

Plate 3.4 : Scanning electron micrographs of (a) Pd-A (b) Pd-B (c) Pd-C (d) Pd-D

Table 3.29
Thermogravimetric analysis of polymer supported Schiff base and catalysts

Compound	Degradation temp. (°C)	Weight loss (%).
8% P(S-DVB) (en-SB)	412.9	47.2
14% P(S-DVB) (en-SB)	394.4	61.1
8% P(S-DVB) (2ap-SB)	378.9	32.7
14% P(S-DVB) (2ap-SB)	408.9	73.8
Pd-A	421.6	41.29
Pd-B	437.5	50.24
Pd-C	425.6	37.34
Pd-D	442.1	45.99

presented in **Tables 3.30 - 3.33**. The effect of various reaction parameters on the rate was studied.

Effect of substrate concentration

The influence of substrate on the rate of hydrogenation of *cis*-cyclooctene was determined at constant palladium concentrations of 4.32×10^{-6} mole for **Pd-A**, 2.76×10^{-6} mole for **Pd-B**, 4.98×10^{-6} mole for **Pd-C** and 3.03×10^{-6} mole for **Pd-D** at 30°C. It was observed that the rate of reaction increased with an increase in substrate concentration [47,48]. The rate of hydrogenation was observed to be slightly higher in case of **Pd-B** and **Pd-D** than for **Pd-A** and **Pd-C**. The order of reaction calculated from the slope of the linear plots of log(initial rate) *vs* log(substrate) is of fractional order with respect to the substrate[49].

Effect of Catalyst Concentration

The variation of catalyst concentration on the rate of hydrogenation was investigated at constant temperature. As expected it was observed that the rate of hydrogenation increased with catalyst concentration but reached an optimum level after about 30 - 45 minutes which may be due to the non-availability of maximum number of active sites at this concentration. An increase in the rate of reaction with an increase in the amount of catalyst was observed [50]. The order of reaction obtained from the slope of the linear plot of log(initial rate) *vs.* log(catalyst concentration) was found to be of fractional order.

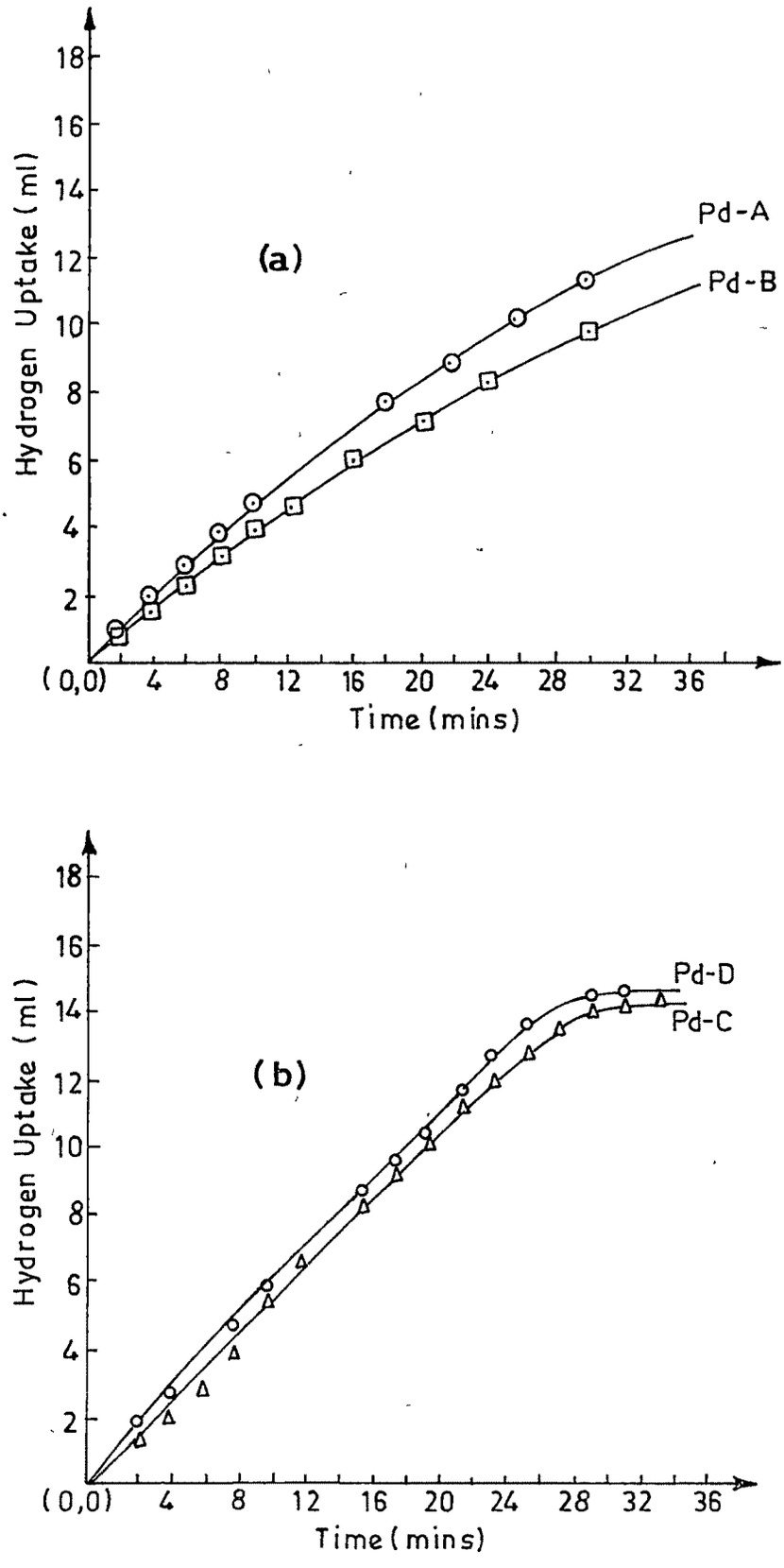

Fig. 3.17. Plots of time *vs* hydrogen uptake in olefin hydrogenation using Pd-catalysts

Table 3.30
Summary of kinetics of hydrogenation of *cis*-cyclooctene for Pd-A

Pd content ($x10^{-6}$mole)	*cis*-cyclooctene ($x10^{-4}$mole)	Temp. (°C)	Rate of Reaction (ml/min.)	E_A Kcal/mole
2.16			0.365	
4.32	1.53	30	0.418	
6.48			0.394	
8.64			0.432	
4.32	0.90	30	0.318	
	2.30		0.497	
	3.63		0.576	
4.32	1.53	25	0.325	
		35	0.432	11.31
		40	0.474	

Reaction Conditions : Solvent = 20ml methanol, $^{p}H_2$*= 1 atmosphere*

Table 3.31:
Summary of kinetics of hydrogenation of *cis*-cyclooctene for Pd-B

Pd content ($x10^{-6}$mole)	*cis*- cyclooctene ($x10^{-4}$ mole)	Temp. (°C)	Rate of Reaction ml/min.	E_A Kcal/mole
1.38			0.357	
2.76	1.53	30	0.472	
4.14			0.512	
5.52			0.636	
2.76	0.90		0.327	
	2.30	30	0.506	
	3.63		0.635	
2.76	1.53	25	0.354	
		35	0.500	5.78
		40	0.673	

Reaction Conditions · Solvent = 20ml methanol, $^{p}H_2 = 1$ *atmosphere*

Table 3.32
Summary of kinetics of hydrogenation of *cis*- cyclooctene for Pd-C

Pd content ($x10^{-6}$ mole)	*cis*-cyclooctene ($x10^{-4}$ mole)	Temp (°C)	Rate of Reaction ml/min.	E_A Kcal/mole
2.39			0.280	
4.78	1.53	30	0.381	
7.17			0.457	
9.56			0.558	
4.78	0.90	30	0.237	
	2.30		0.516	
	3.63		0.637	
4.78	1.53	25	0.300	
		35	0.473	9.78
		40	0.515	

Reaction Conditions : Solvent = 20ml methanol, $^{p}H_2$*= 1 atmosphere*

Table 3.33
Summary of kinetics of hydrogentaion of *cis*-cyclooctene for Pd-D

Pd content ($x10^{-6}$ mole)	*cis*-cyclooctene ($x10^{-4}$ mole)	Temp. (°C)	Rate of Reaction (ml/min.)	E_A Kcal/mole
1.52			0.288	
3.03	1.53	30	0.409	
4.54			0.497	
6.06			0.608	
3.03	0.90	30	0.245	
	2.30		0.545	
	3.63		0.638	
3.03	1.53	25	0.388	
		35	0.474	7.19
		40	0.585	

Reaction Conditions : Solvent = 20ml methanol, $^{p}H_2$ *= 1 atmosphere*

Effect of Temperature

The effect of temperature on the rate of hydrogenation was studied in the range of 25°C to 40°C with a fixed catalyst and substrate concentration. The initial rate of hydrogenation was found to increase with increase in the temperature for all the catalysts. The energy of activation was calculated from the slope of the Arrhenius plots (**Fig 3.18**) and was found to be 11.3 kcal/mole (**Pd-A**), 5.78 kcal/ mole (**Pd-B**), 9.79 kcal/mole (**Pd-C**) and 7.19 kcal/mole for **Pd-D**. The calculated activation energy for the reaction is low compared to the high bond dissociation energy of hydrogen molecule [51-52]. This is attributed to the formation of an intermediate complex with the palladium metal which may provide an alternate low energy path for the reaction.

Effect of Hydrogen Pressure

The influence of hydrogen pressure on the conversion of *cis*-cyclooctene to cyclooctane was studied in the range of 200psi to 400psi at 50°C in a Parr High Pressure Reactor at a constant stirring speed. Similarly, the effect of hydrogen pressure on the hydrogenation of *cis*-cyclooctene at room temperature was studied in the range of 20psi to 40psi in a Parr Hydrogenator (Shaker Type, details in Chapter 2). The data obtained is presented in **Tables 3.34** and **3.35**. From this data, it can be inferred that the conversion of *cis*-cyclooctene to cyclooctane increases with increase in the hydrogen pressure. Kinetic experiments reveal that the initial rate of hydrogenation varies linearly with hydrogen pressure.

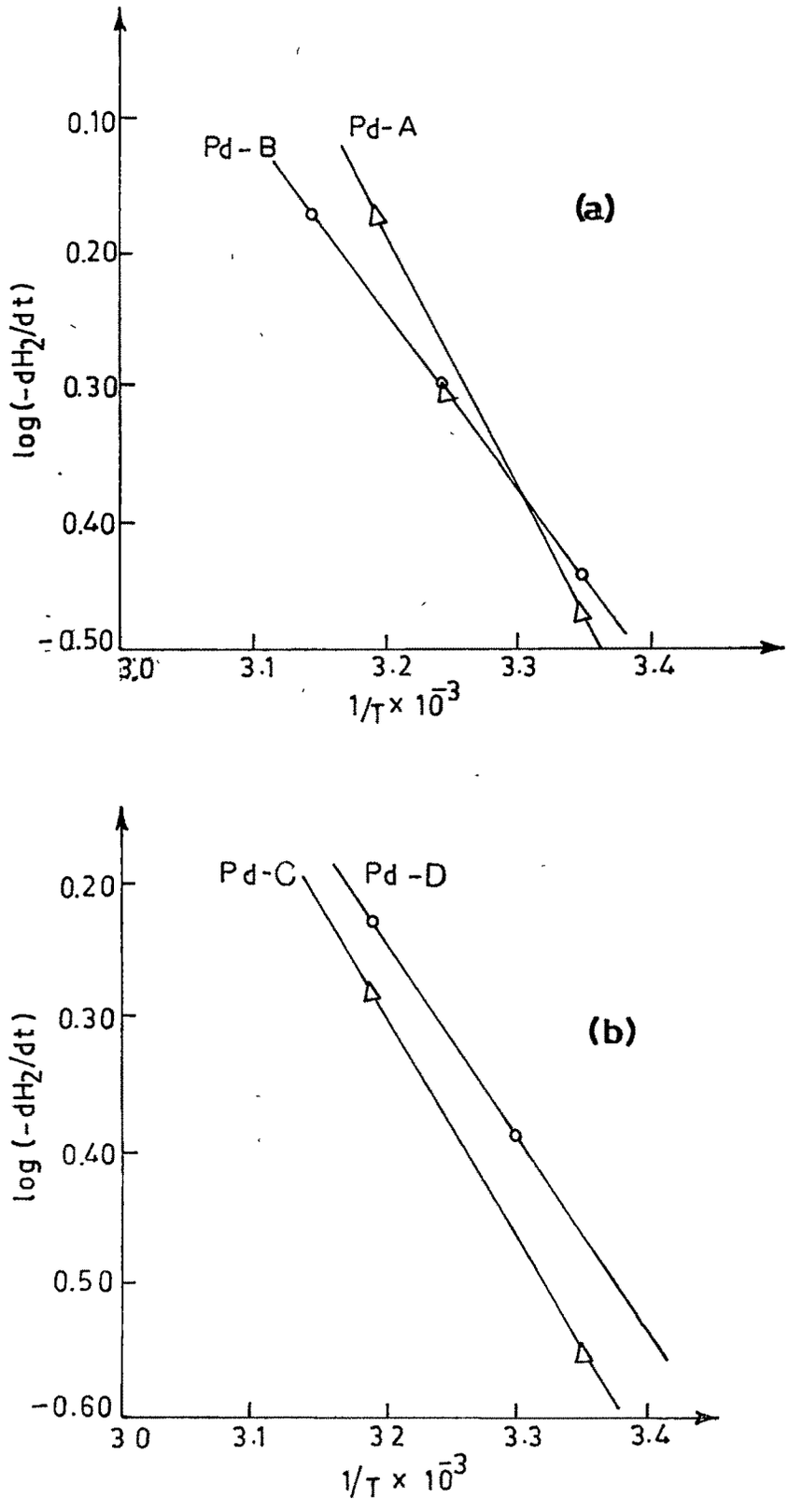

Fig. 3.18. Arrhenius plots of olefin hydrogenation using Pd-catalysts

Table 3.34
Data on the effect of hydrogen pressure at 50°C for polymer supported Pd(II) – Schiff base catalysts[a]

Catalysts	Hydrogen Pressure (psi)	Initial rate of Hydrogenation (ml/min)	Cyclooctane yield (%)[b]
Pd-A	200	0.675	47.7
	300	0.974	54.8
	400	1.420	59.2
Pd-B	200	0.682	49.0
	300	1.020	58.1
	400	1.852	60.5
Pd-C	200	1.762	68.5
	300	2.250	73.1
	400	2.428	78.2
Pd-D	200	1.822	70.1
	300	2.326	75.3
	400	2.276	78.4

[a]*Reaction Conditions : Catalyst weight=100 mg* *Solvent = 20ml methanol*
Cis-cyclooctene=10 mmole *time =4hrs*
Stirrer speed = 150 rpm
[b]*yield based on cis-cyclooctene taken*

Table 3.35
Data on the effect of hydrogen pressure at 27°C for polymer supported Pd(II) – Schiff base catalysts[a]

Catalysts	Hydrogen Pressure (psi)	Cyclooctane yield (%)[b]
Pd-A	20	2.7
	30	6.2
	40	10.1
Pd-B	20	3.1
	30	7.2
	40	10.8
Pd-C	20	7.3
	30	8.1
	40	12.0
Pd-D	20	8.0
	30	9.4
	40	12.8

[a]*Reaction Conditions : Catalyst weight = 100 mg Solvent = 20ml methanol*
Cis-cyclooctene=10 mmole time =24hrs
[b]*yield based on cis-cyclooctene taken*

REFERENCES

[1] S.Schlick, E.Bartet, K.Dyrek, *Acta Polym*, 1, (1996), 47.

[2] K. Nakamoto,*Infrared and Raman spectra of Inorganic and Coordination Compounds Part B · Applications in coordination, organometallic and bioinorganic chemistry*, John Wiley and Sons, Inc, (1997), p.23.

[3] J.R.Thornback, J.R.Wilkinson, *J. Chem. Soc. DaltonTrans.*,(1978), 110.

[4] H.Aneetha, J. Padmaja, P.S.Zacharias, *Polyhedron*, 15, (1996), 2445.

[5] Y.Kurusu, Y Masuyama, M.Saito, S. Saito, *J. Mol Catal.*, 37,(1986), 235.

[6] M.J.Upadhyay, P.K.Bhattacharya, P.A.Ganeshpure, S.Satish, *J.Mol.Catal.*, 73, (1992), 277.

[7] I.Cazaux, C.Caze, *Eur. Poly J*, 29,(1993), 1615.

[8] D.T.Gokak, B.V.Kamath, R.N.Ram, *Indian J Chem.*, 25A,(1986), 1143.

[9] J.O.Turner, J.E.Lyons, *Tetrahedron Lett.*, 29,(1972), 2903.

[10] R.A. Sheldon, *Topics in Curr.Chem.*, 23,(1993), 164.

[11] J.John, M.K.Dalal, R.N.Ram, *J.Mol. Catal. A:Chemical*, 137,(1999), 183.

[12] D.A.Thornton, *Coord.Chem.Rev.* 104,(1990), 251.

[13] A.B.P.Lever, *Inorganic Electronic Spectroscopy*, Elsevier, NewYork, 1984.

[14] J.C.Daram, Y.Jeannin, L.M.Martin, *Inorg.Chem.*, 19,(1980), 2935.

[15] C.R.Jacob, S.P.Varkey, P.Ratnasamy, *Appl. Catal : A.*,168,(1998), 353.

[16] C.Bowers, P.K.Dutta, *J. Catal.*, 122,(1990),271.

[17] P.S.Dixit, K.Srinivasan, *Inorg. Chem.*, 27,(1988), 4507.

[18] B.B.De, B.B.Lohray, S.Sivaram, P.K.Dhal, *Macromolecules*, 27,(1994), 1291.

[19] D.Chatterjee, A.Mitra, *J.Mol Catal.A:Chemical*, 144,(1999), 363.

[20] L.J.Bellamy, Editor. *Infra-red Spectra of Complex Molecules*, London, Chapman & Hall, 1975.

[21] A.S.Kanmani, S.Vancheesan, *J.Mol. Catal.*, 37, (1986), 235.

[22] B.B.De, B.B.Lohray, P.K.Dhal, *Tetrahedron Lett.*, 34,(1993), 2371.

[23] T.S.Reger, K.D.Jande, *J.Am.Chem.Soc.*, 122,(2000),6929.

[24] M.D.Angelino, P.E. Laibinis, *J. Polym Sci A. Polym Chem.*, 37,(1999), 3888

[25] H.Mimoun, *J Mol Catal.*, 7, (1980), 1.

[26] K.B.Sharpless, J.M.Townsend, D.R.Williams, *J.Am.Chem.Soc.*, 94,(1972),295.

[27] R.H.Fish, K.J.Oberhausen, S.Chen, J.F.Richardson, W.Pierce and R.M.Buchanan *Catalysis Letters*, 18,(1993),359.

[28] S.Menage, J.M.Vincent, C.Lambeaux and M.Fontecave, *J.Chem.Soc. Dalton Trans.*, (1994),2081.

[29] R.A.Leising, J.Kim, M.A.Perez and L.Que Jr., *J Am.Chem.Soc.*, 115,(1995),9524.

[30] R.A.Sheldon, J.A.Van Doorn, *J.Catal.*, 31,(1973),427.

[31] R.A.Sheldon in R.Ugo(Ed.) "*Aspects of Homogeneous Catalysis* " D.Reidel, Dordrecht, Vol.4, (1981), 19.

[32] E.S.Gould, R.R.Hiatt, K.C.Irwin, *J.Am.Chem. Soc.*, 90, (1968),4573.

[33] S.Imanura, H.Sasaki, M.Shuno, H.Karai, *J.Catal.*, 117,(1998),72.

[34] S.Leinunen, D.C.Sherrington, A.Sneddon, D.McLoughllin, J.Corker, C. Canevali F.Morazzoni, J.Reedijk, SB.D.Spratt, *J.Catal.*, 183,(1999),251.

[35] P.A.Macfaul, I.W.C.E Arends, K.U.Ingold, D.D.M.Wayner, *J.Am.Chem Soc Perkin Trans.*, 2 , (1997),135.

[36] J.Kim, R.G.Harrison, C.Kim, L.Que Jr., *J Am.Chem Soc.*, 118,(1996),4373.

[37] R.A.Sheldon, J.K.Kochi, *Advan.Catal.*, 25,(1976),343.

[38] J.D.Koola, J.K.Kochi, *J Org.Chem.*, 52,(1987),4545.

[39] R.Barf, R.A.Shelden, *J.Mol.Catal.*, 102,(1995),23.

[40] K.Srinivasan, S.Perrier, J.K.Kochi, *J. Mol Catal.*, 36,(1986),297.

[41] J.N.Shah , R.N.Ram, *J Mol.Catal.*, 77,(1992), 235.

[42] M.K.Dalal, R.N.Ram, *Bull. Mater. Sci.*, 24(2), (2001), 237.

[43] P.S.Hallman, T.A.Stephenson, G.Wilkinson, *Inorganic Synthesis*, 12,(19700, 237.

[44] Sh.Dinkov, M.Arnaudov, *Spectroscopy Letters*, 31(3),(1998), 529.

[45] C.V.Gomes, M.R.Navarro, J.R.Masaquer, *Trans. Met Chem.*, 9, (1984), 52.

[46] M.M. Taquikhan, B. Taquikhan, S. Begum, S. Mustafa Ali, *J. Mol. Catal.* 34 (1986), 283.

[47] Jacob John , Mahesh Dalal, D.R. Patel, R.N. Ram, *J. Macromol. Sci Pure Appl. Chem.*, A 34(3), (1997), 489.

[48] M. Teresawa, K.Kaneda, T. Imanaka, S.Teranishi, *J Catal.*, 51, (1978), 408.

[49] D.T.Gokak, R.N.Ram, *J. Mol Catal.*,49,(1989),285.

[50] S.Arrhenius, *Z.Physik.Chem.*, 4, (1989), 226.

[51] F.Pinna, M.Gonizzi, G.Strukul, G.Cocco, S.Enzo, *J.Catal.*, 82, (1983), 171.

[52] M..Kralik, M.Hronec, S.Lora, G.Palma, M.Zecca, A.Biffis, B.Corain, *J.Mol Catal. A.*, 97, (1995), 145.

" With Time And Patience The Mulberry Leaf
Becomes A Silk Gown "